The contribution of residential coal combustion to atmospheric $PM_{2.5}$ in the North China during winter

Pengfei Liu[1, 3], **Chenglong Zhang**[1, 2, 3], **Chaoyang Xue**[1, 3], **Yujing Mu**[1, 2, 3, 4], **Junfeng Liu**[1, 2, 3], **Yuanyuan Zhang**[1, 2, 3], **Di Tian**[1, 3], **Can Ye**[1, 3], **Hongxing Zhang**[1, 5], **Jian Guan**[6]

[1] Research Center for Eco-Environmental Sciences, Chinese Academy of Sciences, Beijing, 100085, China

[2] Center for Excellence in Urban Atmospheric Environment, Institute of Urban Environment, Chinese Academy of Sciences, Xiamen, 361021, China

[3] University of Chinese Academy of Sciences, Beijing, 100049, China

[4] National Engineering Laboratory for VOCs Pollution Control Material & Technology, University of Chinese Academy of Sciences, Beijing, 100049, China

[5] Beijing Urban Ecosystem Research Station, Beijing, 100085, China

[6] Environment Monitoring Station of Baoding City, Hebei, 071000, China

Correspondence to: Yujing Mu (yjmu@rcees.ac.cn)

Abstract: The vast area in the North China, especially during wintertime, is currently suffering from severe haze events due to the high levels of atmospheric $PM_{2.5}$. To recognize the reasons for the high levels of $PM_{2.5}$, daily samples of $PM_{2.5}$ were simultaneously collected at the four sampling sites of Beijing City (BJ), Baoding City (BD), Wangdu County (WD) and Dongbaituo Countryside (DBT) during the winters and springs of 2014-2015. The concentrations of the typical water-soluble ions (WSIs, such as Cl^-, NO_3^-, SO_4^{2-} and NH_4^+) at DBT were found to be remarkably higher than those at BJ in the two winters, but almost the same as those at BJ in the two springs. The evidently greater concentrations of OC, EC and secondary inorganic ions (NO_3^-, SO_4^{2-}, NH_4^+ and Cl^-) at DBT than at WD, BD and BJ during the winter of 2015 indicated that the pollutants in the rural area were not due to transportation from its neighbor cities but dominated by local emissions. As the distinct source for atmospheric OC and EC in the rural area, the residential coal combustion also made contribution to secondary inorganic ions through the emissions of their precursors (NO_x, SO_2, NH_3 and HCl) as well as heterogeneous or multiphase reactions on the surface of OC and EC. The average mass proportions of OC, EC, NO_3^- and SO_4^{2-} at BD and WD were found to be very close to those at DBT, but evidently different from those at BJ, implying that the pollutants in the cities of WD and BD which are fully surrounded by the countryside were strongly affected by the residential coal combustion. The OC/EC ratios at the four sampling sites were almost the same value (4.8) when the concentrations of $PM_{2.5}$ were greater than 150 μg m^{-3}, suggesting that the residential coal combustion could also make dominant contribution to atmospheric $PM_{2.5}$ at BJ during the severe pollution period when the air parcels were usually from southwest–south regions where high density of farmers reside. The evident increase of the number of the species involved in significant correlations ($p < 0.05$) from the countryside to the cities further confirmed that residential coal combustion was the dominant source for the key species in the rural area and, however, the complex sources including local emissions and regional transportation were responsible for the atmospheric species in the cities. The strong correlations among OC, EC, Cl^-, NO_3^-, and NH_4^+ were found at the four sampling sites but only strong correlation between OC (or EC) and SO_4^{2-} was found at BJ, implying that the formation rate of

SO_4^{2-} via heterogeneous or multiphase reactions might be relatively slower than those of NO_3^-, NH_4^+ and Cl^-. Based on the chemical mass closure (CMC) method, the contributions of the primary particle emission from residential coal combustion to atmospheric $PM_{2.5}$ at BJ, BD, WD and DBT were estimated to be 32 %, 49 %, 43 % and 58 %, respectively.

1 Introduction

In recent years, the vast area in the North China is frequently suffering from severe haze pollution (Chan and Yao, 2008; Zhang et al., 2012; Zhang et al., 2015), which has aroused great attention to the public (Guo et al., 2014; Huang et al., 2014; Cheng et al., 2016; Wang et al., 2016; J. Liu et al., 2016). The severe haze pollution is mainly due to the high level of fine particulate matter with an aerodynamic diameter less than 2.5μm ($PM_{2.5}$) (Huang et al., 2014; P. Liu et al., 2016). $PM_{2.5}$ can reduce atmospheric visibility by absorbing or scattering the incident light (Buseck and Posfai, 1999; Cheng et al., 2006) and increase morbidity and mortality by penetrating the human bronchi and lungs (Nel, 2005; Poschl, 2005; Peplow, 2014).

To alleviate the serious haze pollution problems, the Chinese government has performed a series of control measures for major pollution sources (Zhang et al., 2012; J. Liu et al., 2016; Li et al., 2016b; Wen et al., 2016). For example, coal-fired power plants have been forced to install flue gas desulfurization and denitration (Zhang et al., 2012; Chen et al., 2014), coal has been replaced with natural gas and electricity in megacities (Wang et al., 2009; Duan et al., 2012; Zhao et al., 2013a; Tan et al., 2016), stricter emission standards have been implemented for vehicles and industrial boilers (Zhang et al., 2012; Tang et al., 2016) and so on, resulting in the decrease trend of primary pollutants including $PM_{2.5}$ in recent years (Ma et al., 2016; Wen et al., 2016; Zhang et al., 2016). However, the $PM_{2.5}$ levels can still be larger than 1000 μg m^{-3} in some areas of Beijing-Tianjin-Hebei (BTH) region during the period of the red alert for haze in December 2016 (http://english.mep.gov.cn/News_service/media_news/201612/t20161220_369317.shtml) when

65 the stricter control measures (e.g. stop production for industries and construction, and the odd and
66 even number rule) had been performed (Y. Li et al., 2016), implying that sources other than
67 industries, construction and vehicles might make dominant contribution to atmospheric $PM_{2.5}$ in
68 the region. Residential coal combustion, which is prevailing for heating during winter in the
69 region, was suspected to be a dominant source for atmospheric $PM_{2.5}$. Although annual residential
70 coal consumption (about 42 Tg/year) in BTH region only accounts for small fraction (about 11 %)
71 of the total coal consumption (http://www.qstheory.cn/st/dfst/201306/t20130607_238302.htm), the
72 emission factors of primary pollutants including $PM_{2.5}$ from the residential coal combustion have
73 been found to be about 1-3 orders of magnitude greater than those from coal combustion of
74 industries and power plants (Revuelta et al., 1999; Chen et al., 2005; Xu et al., 2006; Zhang et al.,
75 2008; Geng et al., 2014; Yang et al., 2016). In addition, annual residential coal consumption
76 mainly focuses on the four months in winter. Although the Chinese government has implemented
77 control measures for residential coal combustion (e.g. replacement of traditional coal stoves by
78 new stoves, bituminous coal by anthracite, and coal by electricity and natural gas), the
79 implementation strength of the control measures is still very limited. Additionally, the promoted
80 new stoves are still with strong smoke emission due to lack of clean combustion technique, and
81 the anthracite is not welcomed by farmers because of its extremely slow combustion rate in
82 comparison with bituminous coal.
83 There are few studies focusing on the influence of residential coal combustion on atmospheric
84 particles in the North China. W. Li et al. (2014) concluded that strong sources for PM_{10} in rural
85 residential areas were from household solid fuel combustion, based on annual mean PM_{10}
86 concentrations observed in urban regions (180 ± 171 μg m^{-3}) and rural villages (182 ± 154 μg m^{-3})

87 in the northern China. Duan et al. (2012) inferred that the lower OC/EC ratios at the rural site than
88 at the urban site were ascribed to coal combustion prevailed in the rural area. Our previous study
89 revealed that residential coal combustion made evident contribution to atmospheric water-soluble
90 ions (WSIs) in Beijing (P. Liu et al., 2016). Based on Weather Research and Forecasting model
91 coupled with Chemistry, J. Liu et al. (2016) recently estimated that the residential sources (solid
92 fuel) contributed 32 % and 53 % of the primary $PM_{2.5}$ emissions in the BTH region during the
93 whole year and during the winter of 2010, respectively.
94 In this study, daily samples of $PM_{2.5}$ were simultaneously collected at the four sampling sites
95 (Beijing City, Baoding City, Wangdu County and Dongbaituo Countryside) during the winters and
96 springs of 2014-2015, and the direct evidence for the influence of residential coal combustion on
97 regional $PM_{2.5}$ in the region was found based on the $PM_{2.5}$ levels, $PM_{2.5}$ composition
98 characteristics, correlations among key species in $PM_{2.5}$, back trajectories and chemical mass
99 closure.

100 **2 Materials and methods**

101 **2.1 Sampling sites**

102 The two sampling sites in Beijing City and Dongbaituo Countryside, which have been described
103 in detail by our previous study (P. Liu et al., 2016), were selected on a rooftop (approximately 25
104 m and 5 m above ground, respectively) of the Research Center for Eco-Environmental Sciences,
105 Chinese Academy of Sciences (RCEES, CAS) and a field station in the agricultural field of
106 Dongbaituo village, Baoding, Hebei Province, respectively. Another two sampling sites in
107 Baoding City and Wangdu County were both chosen on the rooftop of local environmental
108 monitor station (about 30 m and 20 m above ground, respectively), which are both located in the

center of the cities and surrounded by some commercial and residential areas. The spatial locations of the four sampling sites are presented in Fig. 1 and the distances between Beijing and Baoding, Baoding and Wangdu, Wangdu and Dongbaituo are about 156 km, 36 km and 12 km, respectively. Thereafter, the sampling sites of Beijing, Baoding, Wangdu and Dongbaituo are abbreviated as BJ, BD, WD and DBT, respectively.

2.2 Sample collection and analysis

$PM_{2.5}$ samples at BJ and DBT were collected simultaneously on PTFE filters (90 mm, Millipore) by medium-volume $PM_{2.5}$ samplers (LaoYing-2034) at a flow rate of 100 L min^{-1} from January 15, 2014 to May 31, 2015, in winter (January 15, 2014-Febrary 25, 2014, November 18, 2014-January 20, 2015 and February 11, 2015-March 15, 2015) and spring (April 21, 2014-May 4, 2014 and March 20, 2015-May 31, 2015). An enhanced observation at BJ, BD, WD and DBT was carried out from January 21 to February 10, 2015 and $PM_{2.5}$ samples were collected in the same way on the quartz fiber filters (90 mm, Munktell). The sampling duration was 24 h (from 15:00 to 15:00 of the following day in local time (UTC + 8)). All the samples were put in the appropriative dishes (90 mm, Millipore) after sampling and preserved in a refrigerator immediately until analysis.

As for the quartz fiber filters, half of each filter was extracted ultrasonically with 10 mL of ultrapure water for half an hour. The solutions were filtered through a micro-porous membrane (pore size, 0.45 μm; diameter, 13 mm) before the analysis, and the WSIs (Cl^-, NO_3^-, SO_4^{2-}, Na^+, NH_4^+, Mg^{2+}, Ca^{2+} and K^+) in the treated filtrates were analyzed by Ion Chromatography (IC, WAYEE IC6200) which has been described in detail by our previous study (P. Liu et al., 2016). A quarter of each filter was cut into fragments and digested with 5 mL 65 % HNO_3 and 2 mL 30 % H_2O_2 (Li et al., 2015) by a microwave digestion system (SINEO, MASTER-40). The digestion

131 solution was diluted to 25 mL with ultrapure water to insure the solution acidity below 10 %, and
132 the trace elements (Al, Mn, Fe, Cu, Zn, As, Se, Sr, Tl and Pb) in the diluted solution were
133 analyzed by a triple-quadrupole inductively coupled plasma mass spectrometry (ICP-MS/MS,
134 Agilent 8800). The standard reference material (GBW07427) was also digested in the same way as
135 the samples and the recoveries of the trace elements were within the allowable ranges of the
136 certified values (100 ± 15 %). Another quarter of each filter was analyzed by a DRI thermal
137 optical carbon analyzer (DRI-2001A) for carbon components (OC and EC). In addition, the PTFE
138 filters were only used for analyzing the WSIs (P. Liu et al., 2016).

139 **2.3 Chemical mass closure**

140 A chemical mass closure (CMC) method was adopted by considering secondary inorganic aerosols
141 (SIA, the sum of SO_4^{2-}, NO_3^- and NH_4^+), sea salt & coal combustion (derived from Cl^- and Na^+),
142 biomass burning (characterized by K^+), mineral dust, EC, primary organic carbon (POC),
143 secondary organic carbon (SOC) and trace element oxide (TEO) (Hsu et al., 2010b; Zhang et al.,
144 2013; Mantas et al., 2014; Tian et al., 2014; Kong et al., 2015).

145 Atmospheric Na^+ and Cl^- were considered to be from sea salt (Brewer, 1975; van Eyk et al., 2011),
146 coal combustion (Bläsing and Müller, 2012; Yu et al., 2013; Wu et al., 2014; He et al., 2015; P. Liu
147 et al., 2016) and biomass burning (Zong et al., 2016; Yao et al., 2016). However, biomass burning
148 in the NCP region is mainly focusing on the harvest seasons in summer and autumn (Zong et al.,
149 2016), and few farmers are currently combusting crop straws for household cooking and heating
150 because of the inconvenience of biomass with respect to coal and liquid gas. Thus, only sea salt
151 and coal combustion were considered for the estimation of mass concentrations for atmospheric
152 Na^+ and Cl^- in this study based on the following equations:

$$[Cl_{cc}^{-}] + [Cl_{ss}^{-}] = [Cl^{-}] \quad (1)$$

$$[Na_{cc}^{+}] + [Na_{ss}^{+}] = [Na^{+}] \quad (2)$$

$$\frac{[Cl_{cc}^{-}]/35.5}{[Na_{cc}^{+}]/23} = 1.4 \quad (3)$$

$$\frac{[Cl_{ss}^{-}]/35.5}{[Na_{ss}^{+}]/23} = 1.18 \quad (4)$$

where $[Cl^-_{ss}]$ and $[Na^+_{ss}]$ are the mass concentrations of Cl^- and Na^+ from sea salt, and $[Cl^-_{cc}]$ and $[Na^+_{cc}]$ are the mass concentrations of Cl^- and Na^+ from coal combustion. The molar ratio of Cl^-_{ss} to Na^+_{ss} was adopted to be 1.18 which represented the typical ratio from sea salt (Brewer, 1975). The molar ratio of Cl^-_{cc} to Na^+_{cc} was chosen to be 1.4 in this study according to our preliminary measurements from the raw bituminous coal prevailed in the North China and the value of 1.4 has been recorded by the previous study (Bläsing and Müller, 2012). If the molar ratios of atmospheric Cl^- to Na^+ in $PM_{2.5}$ were greater than the value of 1.4 or lower than the value of 1.18, atmospheric Cl^- and Na^+ would be considered to be totally from coal combustion or sea salt.

Because the average Al content accounts for about 7 % in mineral dust (Zhang et al., 2003; Ho et al., 2006; Hsu et al., 2010a; Zhang et al., 2013), the mineral dust was estimated based on the follow equation:

$$[Mineral\ dust] = \frac{[Al]}{0.07} \quad (5)$$

POC and SOC were calculated by the EC-tracer OC/EC method (Cheng et al., 2011; Zhao et al., 2013b; G. J. Zheng et al., 2015; Cui et al., 2015) as follows:

$$[POC] = [EC] \times (\frac{[OC]}{[EC]})_{pri} = K[EC] + M \quad (6)$$

$$[SOC] = [OC] - [POC] \quad (7)$$

The values of *K* and *M* are estimated by linear regression analysis using the data pairs with the

lowest 10 % percentile of ambient OC/EC ratios. It should be mentioned that POC could be underestimated and SOC could be overestimated by the EC-tracer OC/EC method, because the lowest 10 % percentile of OC/EC ratios measured were usually less than those from dominant sources of coal combustion and biomass burning in autumn and winter (Ding et al., 2012; Cui et al., 2015).

To estimate the contribution of heavy metal oxide, the enrichment factors (EF) of various heavy metal elements were calculated by the following equation (Hsu et al., 2010b; Zhang et al., 2013):

$$\mathrm{EF} = \frac{\left({}^{[Element]}/_{[Al]}\right)_{aerosol}}{\left({}^{[Element]}/_{[Al]}\right)_{crust}} \quad (8)$$

where $([Element]/[Al])_{aerosol}$ is the ratio of the element to Al in aerosols and $([Element]/[Al])_{crust}$ is the ratio of the element to Al in the average crust (Taylor, 1964). According to the method developed by Landis et al. (2001), the atmospheric concentrations of elements were multiplied by a factor of 0, 0.5 and 1 if their EFs were less than 1, between 1 and 5, and greater than 5, respectively. Based on the EFs (Fig. 2), the equation for estimating TEO was derived as following:

$$[TEO] = 1.3 \times ([Cu] + [Zn] + [Pb] + [As] + [Se] + [Tl] + 0.5 \times [Mn]) \quad (9)$$

The value of 1.3 was the conversion factor of metal abundance to oxide abundance. It should be mentioned that some other elements such as Cd and Ba were not measured in this study, probably resulting in underestimating the proportion of TEO. Nevertheless, the biases are probably insignificant because the proportion of TEO only accounted for less than 2 % in $PM_{2.5}$.

2.4 Meteorological, trace gases and back trajectory

Meteorological data, including wind speed, wind direction, relative humidity (RH), temperature, barometric pressure, as well as air quality index (AQI) based on $PM_{2.5}$, SO_2, NO_2, CO, O_3 at BJ, BD and WD, were obtained from Beijing urban ecosystem research station in RCEES, CAS

196 (http://www.bjurban.rcees.cas.cn/), environmental protection bureau of Baoding City
197 (http://bdhb.gov.cn/) and environmental monitoring station of Wangdu County
198 (http://www.wdx.gov.cn/), respectively. The meteorological data at BJ and BD are shown in Fig. 3
199 and the average concentrations of SO_2 and NO_2 at BJ, BD and WD are listed in Table 2 during the
200 sampling period in the winter of 2015, which will be discussed in section 3.2 and 3.3.
201 The air mass backward trajectories were calculated for 24 h through the National Oceanic and
202 Atmospheric Administration (NOAA) Hybrid Single-Particle Lagrangian Integrated Trajectory
203 Version 4 model (HYSPLIT 4 model) with National Centers for Environmental Prediction's
204 (NCEP) global data. The backward trajectories arriving at 500 m above sampling position were
205 computed at 0:00 h, 6:00 h, 12:00 h and 18:00 h (UTC) for each sampling day. A K-means cluster
206 method was then used for classifying the trajectories into several different clusters and suitable
207 clusters were selected for further analysis.

208 **3 Results and discussion**

209 **3.1 Comparison of atmospheric WSIs between the two sampling sites of BJ and DBT**

210 The daily variations of atmospheric WSIs during the sampling periods at BJ and DBT are shown
211 in Fig. 4. It is evident that the variations of the WSIs between the two sampling sites of BJ and
212 DBT exhibited similar trend, but the mass concentrations of the WSIs were remarkably greater at
213 DBT than at BJ during the two winter seasons. As listed in Table 1, the average concentrations of
214 the typical WSIs were a factor of 1.5-2.0 greater at DBT than at BJ during the two winter seasons,
215 whereas they were approximately the same at the two sampling sites during the two spring seasons.
216 To clearly reveal the differences, the daily D-values (the concentrations of WSIs at DBT minus
217 those at BJ) of several typical WSIs as well as the total WSIs between the two sampling sites of

DBT and BJ are individually illustrated in Fig. 5. With only the exception for Ca^{2+} (typical mineral dust component), the D-values of NH_4^+, NO_3^-, SO_4^{2-} and Cl^- between the two sampling sites of DBT and BJ exhibited positive values during the most sampling days in the two winter seasons, implying that the sources related to mineral dust could be excluded for explaining the obviously higher concentrations of the WSIs at DBT than at BJ. The sampling site of DBT is adjacent to Baoding city where the AQI during the winter always ranked the top three among Chinese cities in recent years (http://113.108.142.147:20035/emcpublish/), and hence the relatively greater concentrations of the WSIs at DBT might be due to the regional pollution. However, the emissions of pollutants from industries, power plants and vehicles are usually relatively stable, which could not account for the remarkable differences in the D-values between the winters and the springs (Fig. 5). If the relatively high concentrations of the WSIs at DBT during the winter were ascribed to the regional pollution, there would be additional strong sources for them in the area of Baoding. To explore whether the regional pollution was responsible for the relatively high concentrations of the WSIs at DBT in winter, the various species in $PM_{2.5}$ collected simultaneously at DBT and its neighbor cities of WD, BD and BJ in the winter of 2015 were further investigated in the following section.

3.2 Daily variations of the species in $PM_{2.5}$ at the four sampling sites

The daily variations of the species in $PM_{2.5}$ at the four sampling sites also exhibited similar trend (Fig. 6), but there were obvious differences ($p < 0.01$) in the concentrations of OC, EC, NH_4^+, NO_3^-, SO_4^{2-}, Cl^- and K^+ among the four sampling sites, ranked in order as BJ < WD < BD < DBT. The meteorological conditions, especially the wind speed and planetary boundary layer (PBL), play pivotal roles in the dispersion and accumulation of atmospheric pollutants (Xu et al., 2011;

240 Tao et al., 2012; Sun et al., 2013; Chen et al., 2015; Gao et al., 2016), which can cause spatial and
241 temporal difference in concentrations of pollutants. As for the sampling sites of BD, WD and DBT,
242 the meteorological conditions could be considered similar because of the short distances (< 36 km)
243 among them, and hence the spatial difference in the concentrations of $PM_{2.5}$ and the major
244 components at the three sampling sites was rationally ascribed to the different source strengths.
245 Although the distance between the sampling sites of BJ and BD is about 156 km, there was no
246 significant difference in the wind speeds between the two sampling sites during the sampling
247 period (1.4 ± 1.4 m/s for BJ and 1.7 ± 1.1 m/s for BD, Fig. 3). Therefore, the spatial difference in
248 the concentrations of $PM_{2.5}$ and the major components between the sampling sites of BJ and the
249 other three could not be ascribed to the difference in the wind speeds. Because the information of
250 PBL was not available in the region of Baoding, it is difficult to discuss the impact of PBL on the
251 spatial difference in the concentrations of the pollutants. As listed in Table 2, the average
252 concentration of the total species at DBT was about a factor of 2.7, 1.8 and 1.4 higher than those
253 at BJ, WD and BD, respectively. The largest levels of the key species in $PM_{2.5}$ at DBT among the
254 four sampling sites implied that the pollutants at the rural site were not through the air parcel
255 transportation from its neighbor cities but mainly ascribed to the local emissions or formation.
256 Vehicles and industries could be rationally excluded for explaining the largest levels of the key
257 species in $PM_{2.5}$ at DBT, because these sources are very sparse in the rural area around DBT (See
258 section 3.4). Compared with the cities, the distinct source for atmospheric pollutants at DBT in
259 winter is the residential coal combustion because residential coal combustion is prevailingly used
260 for heating and cooking in rural areas of the Northern China. The emissions of various pollutants
261 from residential coal combustion were very serious due to the lack of any control measures, as

strong smoke could be seen in the chimney of the residential coal stoves. The emission factors of OC and EC from residential coal combustion were reported to be 0.47-7.82 g kg^{-1} coal and 0.028-2.75 g kg^{-1} coal, respectively (Chen et al., 2005; Zhang et al., 2008). The emission factors of various pollutants from a typical residential coal stove fueled with raw bituminous coal were also investigated in our group according to farmers' customary uses of coal stoves under the alternation cycles of flaming and smoldering (Du et al., 2016; Liu et al., 2017). The emission factors of OC and EC under the entire combustion process can be as high as 10.99 ± 0.95 g kg^{-1} coal and 0.84 ± 0.06 g kg^{-1} coal, respectively (Table 3). Considering the high density of farmers in the rural area, the largest levels of atmospheric OC and EC at DBT could be rationally ascribed to residential coal combustion. However, the proportion of the WSIs from residential coal combustion (Fig. 7a) were extremely low with respect to that of the atmosphere. Therefore, the largest levels of the key WSIs in $PM_{2.5}$ at DBT were suspected to the secondary formation via the heterogeneous or multiphase reactions which might be accelerated by the OC and EC particles (Han et al., 2013; Zhao et al., 2016) emitted from residential coal combustion.

Although the three sampling sites of DBT, WD and BD are closely adjacent, the lowest concentrations of the key species in $PM_{2.5}$ were observed at WD, which was probably ascribed to the replacement of coal with natural gas for the central heating in the county of WD (a main pipe of natural gas is just across the county), e.g., the average concentration of NO_2 was higher at WD than at BD, whereas the average concentration of SO_2 was on the contrary (Table 2).

The city of BD and the county of WD are fully surrounded by countryside with high farmer density, whereas the city of BJ is only neighbored with the countryside in the south-southeast-southwest directions, and thus the residential coal combustion was also suspected

to be responsible for the remarkably higher concentrations of the key species in $PM_{2.5}$ at BD and WD than at BJ. To confirm the above assumptions, the chemical composition and source characteristics of the species in $PM_{2.5}$ were further analyzed in the following section.

3.3 Chemical composition of $PM_{2.5}$ at the four sampling sites

The average mass proportions of the species in $PM_{2.5}$ during the sampling period at the four sampling sites are illustrated in Fig. 7b. OC, EC, NH_4^+, NO_3^- and SO_4^{2-} were found to be the principal species, accounting for about 82 %-88 % of the total species in $PM_{2.5}$ at each sampling site, which were in line with previous studies (Zhao et al., 2013a; X. J. Zhao et al., 2013; Tian et al., 2014; Huang et al., 2014). As for the proportions of individual species, there were obvious differences between the sampling site of BJ and the sampling sites of BD, WD and DBT. The average mass proportions of OC and EC at BD, WD and DBT were very close, accounting for about 45.7 %-47.1 % and 9.0 %-10.4 % of the total species in $PM_{2.5}$, respectively, which were much greater than those (37.9 % for OC and 7.4 % for EC) at BJ. In contrast to OC and EC, the average mass proportions of NO_3^- (10.1 %-10.8 %) and SO_4^{2-} (11.2 %-11.7 %) at BD, WD and DBT were slightly less than those (15.1 % for NO_3^- and 14.0 % for SO_4^{2-}) at BJ, respectively. The obvious differences in the mass proportions of OC, EC, NO_3^- and SO_4^{2-} between the sampling site of BJ and the sampling sites of BD, WD and DBT indicated that the sources for the principal species at BJ were different from the other three sampling sites. The mass proportions of OC, EC, NO_3^- and SO_4^{2-} at BD and WD were very close to those at DBT, implying that residential coal combustion might also be the dominant source for the species in $PM_{2.5}$ at BD and WD. Residential sector (dominated by residential coal combustion) in the region of BTH during winter has been recognized as the dominant source for atmospheric OC and EC (Chen et al., 2017), which was

306 estimated to contribute 85% and 65% of primary OC and EC emissions, respectively (J. Liu et al.,
307 2016). Because the sampling sites of DBT, BD and WD are located in or fully surrounded by high
308 density of countryside, the contribution of residential coal combustion to atmospheric OC and EC
309 at DBT, BD and WD must evidently exceed the regional values estimated by J. Liu et al. (2016).
310 Although the mass proportions of NO_3^- and SO_4^{2-} were evidently lower at BD, WD and DBT than
311 at BJ, the average mass concentrations of NO_3^- and SO_4^{2-} were on the contrary (Table 2).
312 Atmospheric NO_3^- and SO_4^{2-} are mainly from secondary formation via heterogeneous, multiphase
313 or gas-phase reactions which are depended on the concentrations of their precursors (NO_2 and SO_2)
314 and OH radicals, the surface characteristics and areas of particles, and RH (Ravishankara, 1997;
315 Wang et al., 2013; Quan et al., 2014; Nie et al., 2014; He et al., 2014; Yang et al., 2015; B. Zheng
316 et al., 2015). The remarkably higher concentrations of NO_2, SO_2 and $PM_{2.5}$ at BD, WD and DBT
317 (Liu et al., 2015) than at BJ (Table 2) favored secondary formation of NO_3^- and SO_4^{2-}, resulting in
318 the relatively high concentrations of NO_3^- and SO_4^{2-}.
319 As shown in Fig. 8, the serious pollution episodes at BJ usually occurred during the periods with
320 the air parcel from the southwest-south directions where farmers with high density reside, and thus
321 residential coal combustion might also make evident contribution to atmospheric pollutants at BJ.
322 Because the average concentrations of the species in $PM_{2.5}$ were mainly controlled by the highest
323 concentration values and the relatively high concentration level of the species in $PM_{2.5}$ at BJ
324 usually occurred during the serious pollution episodes, the proportions of the species in $PM_{2.5}$
325 were dominated by the serious pollution events. The highest NO_3^- and SO_4^{2-} proportions and the
326 lowest OC and EC proportions at BJ among the four sampling sites might be partly ascribed to the
327 conversions of NO_2 and SO_2 to NO_3^- and SO_4^{2-} during the air parcel transportation from the

328 south-southwest directions. The contribution of the transportation to atmospheric OC and EC at BJ
329 could be verified by the relations between the OC/EC ratios and the $PM_{2.5}$ levels (Fig. 9). The
330 OC/EC ratios (about 4.9 ± 0.7) at WD and DBT were almost independent of the $PM_{2.5}$ levels,
331 whereas the OC/EC ratios at BJ and BD remarkably decreased with increasing the $PM_{2.5}$ levels
332 and reached the almost same value (about 4.8 ± 0.5) as those at WD and DBT when the
333 concentrations of $PM_{2.5}$ were above 150 μg m^{-3} (the serious pollution events). Because there were
334 relatively sparse emissions from vehicles and industries at WD and DBT, the almost constant of
335 OC/EC ratios under the different levels of $PM_{2.5}$ at WD and DBT further revealed that
336 atmospheric OC and EC were dominated by the local residential coal combustion. The almost
337 same OC/EC ratios at the four sampling sites with the concentrations of $PM_{2.5}$ greater than 150 μg
338 m^{-3} indicated that the residential coal combustion also made a dominant contribution to
339 atmospheric OC and EC in the two cities during the severe pollution period. Our previous study
340 (C. Liu et al., 2016) also found that the contribution from residential coal combustion to
341 atmospheric VOCs increased from 23 % to 33 % with increasing pollution levels in Beijing.
342 It should be mentioned that the OC/EC ratios observed at DBT and WD were about a factor of 2.7
343 less than that (13.1) of the emission from the residential coal combustion and, however, the
344 OC/EC ratios observed at BJ and BD were too high to be explained by direct emissions from
345 diesel (0.4-0.8) and gasoline (3.1) vehicles (Shah et al., 2004; Geller et al., 2006). The OC emitted
346 from the residential coal combustion might be easily degraded or volatilized in the atmosphere,
347 resulting in the relatively low OC/EC ratios observed at DBT and WD. In China, aromatic
348 compounds as typical pollutants from vehicle emissions are very reactive, favoring secondary
349 organic aerosols (SOA) formation (Zhang et al., 2017), which was suspected to make evident

contribution to the OC/EC ratios at BJ and BD when the atmospheric EC concentrations were relatively low. For example, the extremely high OC/EC ratios (> 6.0) at BJ and BD only occurred when the atmospheric EC concentrations were less than 3.2 μg m^{-3} at BJ and 5.4 μg m^{-3} at BD. Because the atmospheric EC concentrations at BJ and BD were about a factor of 4-6 greater during the serious pollution events than during the slight pollution events, the effect of SOA formation on the OC/EC ratios would be smaller during the serious pollution events if the SOA formation rate kept constant.

3.4 Correlations among the species in $PM_{2.5}$

The correlations among the WSIs, OC and EC in $PM_{2.5}$ at the four sampling sites are listed in Table 4. The number of the species involved in significant correlations ($p < 0.05$) evidently increased from the countryside to the cities and was 18, 28, 30 and 36 at DBT, WD, BD and BJ, respectively. The significant correlations among the species could be classified as three types: 1) associated with OC and EC; 2) associated with Ca^{2+} and Mg^{2+}; and 3) associated with K^+. Three types of significant correlations at DBT were independent of each other, whereas they were involved in interrelation more and more from WD to BJ. The independence for the three types of significant correlations at DBT further confirmed that residential coal combustion was preferentially dominant source for atmospheric OC and EC. The strong correlations among OC, EC, NO_3^-, NH_4^+ and Cl^- at DBT indicated that the OC and EC emitted from the residential coal combustion could quickly accelerate secondary formation of NO_3^-, NH_4^+ and Cl^- via heterogeneous or multiphase reactions of NO_x, NH_3 and HCl which have been verified to be emitted from the residential coal combustion (Wang et al., 2005; Shapiro et al., 2007; Bläsing and Müller, 2010; Meng et al., 2011; Zhang et al., 2013; Gao et al., 2015; Li et al., 2016a; Huang et al.,

2016). The interrelation for the three types of significant correlations at WD, BD and BJ implied that complex sources including local emissions and regional transportation were dominant for atmospheric species in the cities. The species associated with Ca^{2+} and Mg^{2+} from construction and road dust (Liang et al., 2016) as well as the species associated with K^+ from biomass (municipal solid waste) burning (Gao et al., 2011; J. Li et al., 2014; Yao et al., 2016) in the cities would accumulate under stagnant air conditions at the earth surface, meanwhile the OC and EC concentrations could also increase due to the air parcel transportation with abundant OC and EC in the upper layer from the south-southwest directions (Fig. 8). It is interesting to note that the strong correlations among OC, EC, NO_3^-, NH_4^+ and Cl^- were found at the four sampling sites, whereas the strong correlation between OC (or EC) and SO_4^{2-} was only found at BJ. Because the sampling sites of DBT, WD and BD are close to the source of OC and EC from the residential coal combustion, the strong correlations among OC, EC, NO_3^-, NH_4^+ and Cl^- but the non-existent correlation between OC (or EC) and SO_4^{2-} implied that the formation rate of SO_4^{2-} via heterogeneous or multiphase reactions might be relatively slower than those of NO_3^-, NH_4^+ and Cl^-. The reactive uptake coefficients of SO_2 oxidation by O_3 have been reported to be from 4.3×10^{-8} to 7×10^{-7} on different mineral aerosols and from 1×10^{-6} to 6×10^{-6} on soot particles (Wu et al., 2011; Song et al., 2012), which is at least one order of magnitude less than those of NO_2 (1.03×10^{-2}-3.43×10^{-3} on soot particles and 1.03×10^{-6}-1.2×10^{-5} on mineral aerosols) (Underwood et al., 2001; Esteve et al., 2004; Ma et al., 2011; Ma et al., 2017). The OC, EC and SO_2 emitted from the residential coal combustion experienced the relatively long period of excursion to be transported to Beijing, resulting in the strong correlation between OC (or EC) and SO_4^{2-} at BJ.

As listed in Table 5, the pronounced correlations for [As] vs. [Se] and [Cu] vs. [Zn] at the four

394 sampling sites indicated that the two pairs of elements were from the common sources. Based on
395 the remarkable elevations of As and Se near a coal-fired power plant with respect to the
396 background site, Jayasekher (2009) pointed out that their significant correlation can be used as the
397 tracer for coal combustion. Because Cu and Zn have been found to be mainly released from the
398 additives of vehicle lubricating oils, brake and tire wear during transportation activities (Yu et al.,
399 2013; Zhang et al., 2013; Tan et al., 2016), their significant correlation has been used as the tracer
400 for vehicle emissions. Both coal combustion and vehicle emissions could make contribution to
401 atmospheric Pb (Zhang et al., 2013; Gao et al., 2016), and thus the correlations for [Pb] vs.
402 [Cu+Zn] and [Pb] vs. [As+Se] could reflect their local dominant sources. As shown in Fig. 10, the
403 moderately strong correlation between [Pb] and [Cu+Zn] but non-existent correlation between [Pb]
404 and [As+Se] were found at BJ, whereas the correlations at the rural site of DBT were on the
405 contrary, indicating that atmospheric Pb, Cu and Zn at BJ were mainly related to the vehicle
406 emissions and atmospheric Pb, As and Se at DBT were dominated by residential coal combustion.
407 Because the sampling sites of BD and WD were affected by both vehicle emissions and residential
408 coal combustion, the moderately strong correlations between [Pb] and [Cu+Zn] as well as [Pb]
409 and [As+Se] were found at the two sampling sites. Although there was non-existent correlation
410 between [Pb] and [As+Se] at BJ, the contribution of residential coal combustion to atmospheric
411 $PM_{2.5}$ in the city of BJ could not be excluded because the trace elements from coal combustion are
412 mainly present in relatively large particles (0.8-2.5 μm) which might quickly deposit near their
413 sources (Wang et al., 2008).

414 **3.5 Source apportionment of $PM_{2.5}$ at the four sampling sites**

415 The source characteristics of $PM_{2.5}$ at the four sampling sites were analyzed by the CMC method

which has been described in detail in section 2.3. The average proportions of the species from different sources in $PM_{2.5}$ during the sampling period at the four sampling sites are comparatively shown in Fig. 11. It is evident that secondary aerosols (SIA + SOC) accounted for the largest proportion (about 32-41 %) in $PM_{2.5}$, followed by POC (about 24-28 %), EC (about 6-8 %), mineral dust (about 2-8 %) and Cl^-_{cc} (about 2-5 %) at the four sampling sites. The proportion of mineral dust was the highest at BJ and the lowest at DBT among the four sampling sites, whereas the proportion of Cl^-_{cc} was on the contrary. Because the concentrations of the mineral dust compounds were much higher under stagnant weather condition than under clean days at BJ, the remarkably high proportion of mineral dust at BJ was mainly ascribed to the emissions from road dust and construction (Liang et al., 2016) during the sampling period. The obviously high proportion of Cl^-_{cc} at DBT was ascribed to the emission from residential coal combustion (Shen et al., 2016). In addition, the proportions of TEO, K^+_{bb} and Cl^-_{ss} were less than about 2 %, which were insignificant to the sources of $PM_{2.5}$ at the four sampling sites during the sampling period.

Atmospheric Primary Organic Matters (POM) and Cl^-_{cc} at the four sampling sites could be estimated based on POM≈POC × 1.6 (Cheung et al., 2005; Hsu et al., 2010b; Han et al., 2015) and the formulas (1)-(4), respectively. The sum of POM, EC and Cl^-_{cc} at DBT was assumed to be solely from residential coal combustion, accounting for about 58% in $PM_{2.5}$ (Fig. 12). Assuming that the ratio of Cl^-_{cc} to the sum of POM, EC and Cl^-_{cc} was constant for coal combustion at the four sampling sites, the primary contribution of coal combustion to atmospheric $PM_{2.5}$ at BJ, BD and WD could be estimated to be 32 %, 49 % and 43 % (Fig. 12), respectively. The annual residential coal consumption mainly focused on the four months in winter, accounting for about 11 % of the total coal consumption in the region of BTH. Because the emission factor of $PM_{2.5}$ from

residential coal combustion (about 1054-12910 mg kg^{-1}) was about 1-3 orders of magnitude greater than those from industry boilers or coal power plants (about 16-100 mg kg^{-1}) (Chen et al., 2005; Zhang et al., 2008), the estimated proportions of the contribution of coal combustion to atmospheric $PM_{2.5}$ at the four sampling sites during the winter were mainly ascribed to residential coal combustion. If the primary $PM_{2.5}$ was only considered, the contribution of residential coal combustion to the primary $PM_{2.5}$ at BJ would achieve to be about 59 %, which was in line with the value of 57 % estimated by J. Liu et al. (2016) for the winter of 2010 in Beijing.

4 Conclusions

Based on the comprehensive analysis of the levels, composition characteristics, the correlations of the key species in $PM_{2.5}$ and the back trajectories, residential coal combustion in the North China during winter was found not only to be the dominant source for atmospheric OC, EC, Cl^-, NO_3^-, SO_4^{2-} and NH_4^+ in rural areas but also to make evident contribution to the species in cities. According to the CMC method, the contributions of the primary particle emission from residential coal combustion to atmospheric $PM_{2.5}$ at BJ, BD, WD and DBT during winter were estimated to be 32 %, 49 %, 43 % and 58 %, respectively. Therefore, strict control measures should be implemented for the emissions from residential coal combustion to mitigate the currently serious $PM_{2.5}$ pollution during the winter in the North China.

Author contribution

Y. J. Mu designed the experiments and prepared the manuscript. **P. F. Liu** and **C. L. Zhang** carried out the experiments and prepared the manuscript, and contributed equally to this work. **C. Y. Xue** carried out the experiments. **J. F. Liu**, **Y. Y. Zhang**, **D. Tian** and **C. Ye** were involved in part of the work. **H. X. Zhang** provided the meteorological data and trace gases in Beijing. **J.**

Guan provided the meteorological data and trace gases in Baoding and Wangdu.

Acknowledgements

This work was supported by the National Natural Science Foundation of China (No. 21477142, 91544211 and 41575121), the Special Fund for Environmental Research in the Public Interest (No. 201509002) and the projects of the Strategic Priority Research Program (B) of the Chinese Academy of Sciences (No. XDB05010100). We sincerely thank Dr. Dawei Lu and Dr. Chengbin Liu from Prof. Guibin Jiang group (RCEES) for their support in trace elements analysis.

References

Bläsing, M., and Müller, M.: Mass spectrometric investigations on the release of inorganic species during gasification and combustion of German hard coals, Combustion and Flame, 157, 1374-1381, 10.1016/j.combustflame.2010.01.003, 2010.

Bläsing, M., and Müller, M.: Release of Alkali Metal, Sulfur, and Chlorine Species during High-Temperature Gasification of Coal and Coal Blends in a Drop Tube Reactor, Energy & Fuels, 26, 6311-6315, 10.1021/ef301205j, 2012.

Brewer, P. G. (Eds.): Minor elements in sea water, Chemical Oceanography, Academic, San Diego, California, 1975.

Buseck, P. R., and Posfai, M.: Airborne minerals and related aerosol particles: Effects on climate and the environment, Proceedings of the National Academy of Sciences of the United States of America, 96, 3372-3379, 10.1073/pnas.96.7.3372, 1999.

Chan, C. K., and Yao, X.: Air pollution in mega cities in China, Atmospheric Environment, 42, 1-42, 10.1016/j.atmosenv.2007.09.003, 2008.

Chen, C., Sun, Y. L., Xu, W. Q., Du, W., Zhou, L. B., Han, T. T., Wang, Q. Q., Fu, P. Q., Wang, Z. F., Gao, Z. Q., Zhang, Q., and Worsnop, D. R.: Characteristics and sources of submicron aerosols above the urban canopy (260 m) in Beijing, China, during the 2014 APEC summit, Atmospheric Chemistry and Physics, 15, 12879-12895, 10.5194/acp-15-12879-2015, 2015.

Chen, L. H., Sun, Y. Y., Wu, X. C., Zhang, Y. X., Zheng, C. H., Gao, X., and Cen, K.: Unit-based emission inventory and uncertainty assessment of coal-fired power plants, Atmospheric Environment, 99, 527-535, 10.1016/j.atmosenv.2014.10.023, 2014.

Chen, S., Xu, L., Zhang, Y., Chen, B., Wang, X., Zhang, X., Zheng, M., Chen, J., Wang, W., Sun, Y., Fu, P., Wang, Z., and Li, W.: Direct observations of organic aerosols in common wintertime hazes in North China: insights into direct emissions from Chinese residential stoves, Atmospheric Chemistry and Physics, 17, 1259-1270, 10.5194/acp-17-1259-2017, 2017.

Chen, Y. J., Sheng, G. Y., Bi, X. H., Feng, Y. L., Mai, B. X., and Fu, J. M.: Emission factors for carbonaceous particles and polycyclic aromatic hydrocarbons from residential coal combustion in China, Environ. Sci. Technol., 39, 1861-1867, 10.1021/es0493650, 2005.

Cheng, Y., He, K. B., Duan, F. K., Zheng, M., Du, Z. Y., Ma, Y. L., and Tan, J. H.: Ambient

organic carbon to elemental carbon ratios: Influences of the measurement methods and implications, Atmospheric Environment, 45, 2060-2066, 10.1016/j.atmosenv.2011.01.064, 2011.
Cheng, Y., Zheng, G., Wei, C., Mu, Q., Zheng, B., Wang, Z., Gao, M., Zhang, Q., He, K., Carmichael, G., Pöschl, U., and Su, H.: Reactive nitrogen chemistry in aerosol water as a source of sulfate during haze events in China, Science Advances, 2, 10.1126/sciadv.1601530, 2016.
Cheng, Y. F., Eichler, H., Wiedensohler, A., Heintzenberg, J., Zhang, Y. H., Hu, M., Herrmann, H., Zeng, L. M., Liu, S., Gnauk, T., Brüggemann, E., and He, L. Y.: Mixing state of elemental carbon and non-light-absorbing aerosol components derived from in situ particle optical properties at Xinken in Pearl River Delta of China, Journal of Geophysical Research, 111, 10.1029/2005jd006929, 2006.
Cheung, H. C., Wang, T., Baumann, K., and Guo, H.: Influence of regional pollution outflow on the concentrations of fine particulate matter and visibility in the coastal area of southern China, Atmospheric Environment, 39, 6463-6474, 10.1016/j.atmosenv.2005.07.033, 2005.
Cui, H., Mao, P., Zhao, Y., Nielsen, C. P., and Zhang, J.: Patterns in atmospheric carbonaceous aerosols in China: emission estimates and observed concentrations, Atmospheric Chemistry and Physics, 15, 8657-8678, 10.5194/acp-15-8657-2015, 2015.
Ding, X., Wang, X. M., Gao, B., Fu, X. X., He, Q. F., Zhao, X. Y., Yu, J. Z., and Zheng, M.: Tracer-based estimation of secondary organic carbon in the Pearl River Delta, south China, Journal of Geophysical Research: Atmospheres, 117, D05313, 10.1029/2011jd016596, 2012.
Du, Q., Zhang, C., Mu, Y., Cheng, Y., Zhang, Y., Liu, C., Song, M., Tian, D., Liu, P., Liu, J., Xue, C., and Ye, C.: An important missing source of atmospheric carbonyl sulfide: Domestic coal combustion, Geophysical Research Letters, 43, 8720-8727, 10.1002/2016gl070075, 2016.
Duan, J., Tan, J., Wang, S., Chai, F., He, K., and Hao, J.: Roadside, Urban, and Rural comparison of size distribution characteristics of PAHs and carbonaceous components of Beijing, China, Journal of Atmospheric Chemistry, 69, 337-349, 10.1007/s10874-012-9242-5, 2012.
Esteve, W., Budzinski, H., and Villenave, E.: Relative rate constants for the heterogeneous reactions of OH, NO_2 and NO radicals with polycyclic aromatic hydrocarbons adsorbed on carbonaceous particles. Part 1: PAHs adsorbed on 1–2μm calibrated graphite particles, Atmospheric Environment, 38, 6063-6072, 10.1016/j.atmosenv.2004.05.059, 2004.
Gao, J., Tian, H., Cheng, K., Lu, L., Zheng, M., Wang, S., Hao, J., Wang, K., Hua, S., Zhu, C., and Wang, Y.: The variation of chemical characteristics of $PM_{2.5}$ and PM_{10} and formation causes during two haze pollution events in urban Beijing, China, Atmospheric Environment, 107, 1-8, 10.1016/j.atmosenv.2015.02.022, 2015.
Gao, J., Peng, X., Chen, G., Xu, J., Shi, G. L., Zhang, Y. C., and Feng, Y. C.: Insights into the chemical characterization and sources of $PM_{2.5}$ in Beijing at a 1-h time resolution, The Science of the total environment, 542, 162-171, 10.1016/j.scitotenv.2015.10.082, 2016.
Gao, M., Carmichael, G. R., Wang, Y., Saide, P. E., Yu, M., Xin, J., Liu, Z., and Wang, Z.: Modeling study of the 2010 regional haze event in the North China Plain, Atmospheric Chemistry and Physics, 16, 1673-1691, 10.5194/acp-16-1673-2016, 2016.
Gao, X., Yang, L., Cheng, S., Gao, R., Zhou, Y., Xue, L., Shou, Y., Wang, J., Wang, X., Nie, W., Xu, P., and Wang, W.: Semi-continuous measurement of water-soluble ions in $PM_{2.5}$ in Jinan, China: Temporal variations and source apportionments, Atmospheric Environment, 45, 6048-6056, 10.1016/j.atmosenv.2011.07.041, 2011.
Geller, M. D., Ntziachristos, L., Mamakos, A., Samaras, Z., Schmitz, D. A., Froines, J. R., and

Sioutas, C.: Physicochemical and redox characteristics of particulate matter (PM) emitted from gasoline and diesel passenger cars, Atmospheric Environment, 40, 6988-7004, 10.1016/j.atmosenv.2006.06.018, 2006.
Geng, C., Chen, J., Yang, X., Ren, L., Yin, B., Liu, X., and Bai, Z.: Emission factors of polycyclic aromatic hydrocarbons from domestic coal combustion in China, Journal of Environmental Sciences, 26, 160-166, 10.1016/s1001-0742(13)60393-9, 2014.
Guo, S., Hu, M., Zamora, M. L., Peng, J., Shang, D., Zheng, J., Du, Z., Wu, Z., Shao, M., Zeng, L., Molina, M. J., and Zhang, R.: Elucidating severe urban haze formation in China, Proceedings of the National Academy of Sciences of the United States of America, 111, 17373-17378, 10.1073/pnas.1419604111, 2014.
Han, C., Liu, Y., and He, H.: Role of organic carbon in heterogeneous reaction of NO_2 with soot, Environ Sci Technol, 47, 3174-3181, 10.1021/es304468n, 2013.
Han, T., Liu, X., Zhang, Y., Qu, Y., Zeng, L., Hu, M., and Zhu, T.: Role of secondary aerosols in haze formation in summer in the Megacity Beijing, J Environ Sci (China), 31, 51-60, 10.1016/j.jes.2014.08.026, 2015.
He, H., Wang, Y., Ma, Q., Ma, J., Chu, B., Ji, D., Tang, G., Liu, C., Zhang, H., and Hao, J.: Mineral dust and NO_x promote the conversion of SO_2 to sulfate in heavy pollution days, Scientific reports, 4, 4172, 10.1038/srep04172, 2014.
He, Y., Qiu, K. Z., Whiddon, R., Wang, Z. H., Zhu, Y. Q., Liu, Y. Z., Li, Z. S., and Cen, K. F.: Release characteristic of different classes of sodium during combustion of Zhun-Dong coal investigated by laser-induced breakdown spectroscopy, Science Bulletin, 60, 1927-1934, 2015.
Ho, K. F., Lee, S. C., Cao, J. J., Chow, J. C., Watson, J. G., and Chan, C. K.: Seasonal variations and mass closure analysis of particulate matter in Hong Kong, The Science of the total environment, 355, 276-287, 10.1016/j.scitotenv.2005.03.013, 2006.
Hsu, S. C., Liu, S. C., Arimoto, R., Shiah, F. K., Gong, G. C., Huang, Y. T., Kao, S. J., Chen, J. P., Lin, F. J., Lin, C. Y., Huang, J. C., Tsai, F., and Lung, S. C. C.: Effects of acidic processing, transport history, and dust and sea salt loadings on the dissolution of iron from Asian dust, Journal of Geophysical Research, 115, 10.1029/2009jd013442, 2010a.
Hsu, S. C., Liu, S. C., Tsai, F., Engling, G., Lin, I. I., Chou, C. K. C., Kao, S. J., Lung, S. C. C., Chan, C. Y., Lin, S. C., Huang, J. C., Chi, K. H., Chen, W. N., Lin, F. J., Huang, C. H., Kuo, C. L., Wu, T. C., and Huang, Y. T.: High wintertime particulate matter pollution over an offshore island (Kinmen) off southeastern China: An overview, Journal of Geophysical Research, 115, 10.1029/2009jd013641, 2010b.
Huang, R. J., Zhang, Y., Bozzetti, C., Ho, K. F., Cao, J. J., Han, Y., Daellenbach, K. R., Slowik, J. G., Platt, S. M., Canonaco, F., Zotter, P., Wolf, R., Pieber, S. M., Bruns, E. A., Crippa, M., Ciarelli, G., Piazzalunga, A., Schwikowski, M., Abbaszade, G., Schnelle-Kreis, J., Zimmermann, R., An, Z., Szidat, S., Baltensperger, U., El Haddad, I., and Prevot, A. S.: High secondary aerosol contribution to particulate pollution during haze events in China, Nature, 514, 218-222, 10.1038/nature13774, 2014.
Huang, X., Liu, Z., Zhang, J., Wen, T., Ji, D., and Wang, Y.: Seasonal variation and secondary formation of size-segregated aerosol water-soluble inorganic ions during pollution episodes in Beijing, Atmospheric Research, 168, 70-79, 10.1016/j.atmosres.2015.08.021, 2016.
Jayasekher, T.: Aerosols near by a coal fired thermal power plant: chemical composition and toxic evaluation, Chemosphere, 75, 1525-1530, 10.1016/j.chemosphere.2009.02.001, 2009.

584 Kong, S. F., Li, L., Li, X. X., Yin, Y., Chen, K., Liu, D. T., Yuan, L., Zhang, Y. J., Shan, Y. P., and
585 Ji, Y. Q.: The impacts of firework burning at the Chinese Spring Festival on air quality: insights of
586 tracers, source evolution and aging processes, Atmospheric Chemistry and Physics, 15, 2167-2184,
587 10.5194/acp-15-2167-2015, 2015.
588 Landis, M. S., Norris, G. A., Williams, R. W., and Weinstein, J. P.: Personal exposures to $PM_{2.5}$
589 mass and trace elements in Baltimore, MD, USA, Atmospheric Environment, 35, 6511-6524,
590 10.1016/s1352-2310(01)00407-1, 2001.
591 Li, J., Song, Y., Mao, Y., Mao, Z., Wu, Y., Li, M., Huang, X., He, Q., and Hu, M.: Chemical
592 characteristics and source apportionment of $PM_{2.5}$ during the harvest season in eastern China's
593 agricultural regions, Atmospheric Environment, 92, 442-448, 10.1016/j.atmosenv.2014.04.058,
594 2014.
595 Li, Q., Jiang, J. K., Cai, S. Y., Zhou, W., Wang, S. X., Duan, L., and Hao, J. M.: Gaseous
596 Ammonia Emissions from Coal and Biomass Combustion in Household Stoves with Different
597 Combustion Efficiencies, Environmental Science & Technology Letters, 3, 98-103,
598 10.1021/acs.estlett.6b00013, 2016a.
599 Li, Q., Li, X., Jiang, J., Duan, L., Ge, S., Zhang, Q., Deng, J., Wang, S., and Hao, J.: Semi-coke
600 briquettes: towards reducing emissions of primary $PM_{2.5}$, particulate carbon, and carbon monoxide
601 from household coal combustion in China, Scientific reports, 6, 19306, 10.1038/srep19306,
602 2016b.
603 Li, T., Wang, Y., Li, W. J., Chen, J. M., Wang, T., and Wang, W. X.: Concentrations and solubility
604 of trace elements in fine particles at a mountain site, southern China: regional sources and cloud
605 processing, Atmospheric Chemistry and Physics, 15, 8987-9002, 10.5194/acp-15-8987-2015,
606 2015.
607 Li, W., Wang, C., Wang, H., Chen, J., Yuan, C., Li, T., Wang, W., Shen, H., Huang, Y., Wang, R.,
608 Wang, B., Zhang, Y., Chen, H., Chen, Y., Tang, J., Wang, X., Liu, J., Coveney, R. M., Jr., and Tao,
609 S.: Distribution of atmospheric particulate matter (PM) in rural field, rural village and urban areas
610 of northern China, Environ Pollut, 185, 134-140, 10.1016/j.envpol.2013.10.042, 2014.
611 Li, Y., Ye, C., Liu, J., Zhu, Y., Wang, J., Tan, Z., Lin, W., Zeng, L., and Zhu, T.: Observation of
612 regional air pollutant transport between the megacity Beijing and the North China Plain,
613 Atmospheric Chemistry and Physics, 16, 14265-14283, 10.5194/acp-16-14265-2016, 2016.
614 Liang, C. S., Duan, F. K., He, K. B., and Ma, Y. L.: Review on recent progress in observations,
615 source identifications and countermeasures of $PM_{2.5}$, Environ Int, 86, 150-170,
616 10.1016/j.envint.2015.10.016, 2016.
617 Liu, C., Mu, Y., Liu, J., Zhang, C., Zhang, Y., Liu, P., and Zhang, H.: The levels, variation
618 characteristics and sources of atmospheric non-methane hydrocarbon compounds during
619 wintertime in Beijing, China, Atmos. Chem. Phys. Discuss., 2016, 1-23, 10.5194/acp-2016-783,
620 2016.
621 Liu, C., Zhang, C., Mu, Y., Liu, J., and Zhang, Y.: Emission of volatile organic compounds from
622 domestic coal stove with the actual alternation of flaming and smoldering combustion processes,
623 Environ Pollut, 221, 385-391, 10.1016/j.envpol.2016.11.089, 2017.
624 Liu, J., Mauzerall, D. L., Chen, Q., Zhang, Q., Song, Y., Peng, W., Klimont, Z., Qiu, X. H., Zhang,
625 S. Q., Hu, M., Lin, W. L., Smith, K. R., and Zhu, T.: Air pollutant emissions from Chinese
626 households: A major and underappreciated ambient pollution source, Proceedings of the National
627 Academy of Sciences of the United States of America, 113, 7756-7761, 10.1073/pnas.1604537113,

2016.
Liu, K., Zhang, C., Cheng, Y., Liu, C., Zhang, H., Zhang, G., Sun, X., and Mu, Y.: Serious BTEX pollution in rural area of the North China Plain during winter season, J Environ Sci (China), 30, 186-190, 10.1016/j.jes.2014.05.056, 2015.
Liu, P., Zhang, C., Mu, Y., Liu, C., Xue, C., Ye, C., Liu, J., Zhang, Y., and Zhang, H.: The possible contribution of the periodic emissions from farmers' activities in the North China Plain to atmospheric water-soluble ions in Beijing, Atmospheric Chemistry and Physics, 16, 10097-10109, 10.5194/acp-16-10097-2016, 2016.
Ma, J., Liu, Y., and He, H.: Heterogeneous reactions between NO_2 and anthracene adsorbed on SiO_2 and MgO, Atmospheric Environment, 45, 917-924, 10.1016/j.atmosenv.2010.11.012, 2011.
Ma, Q., Wang, T., Liu, C., He, H., Wang, Z., Wang, W., and Liang, Y.: SO_2 Initiates the Efficient Conversion of NO_2 to HONO on MgO Surface, Environ. Sci. Technol., 51, 3767-3775, 10.1021/acs.est.6b05724, 2017.
Ma, Z. W., Hu, X. F., Sayer, A. M., Levy, R., Zhang, Q., Xue, Y. G., Tong, S. L., Bi, J., Huang, L., and Liu, Y.: Satellite-Based Spatiotemporal Trends in $PM_{2.5}$ Concentrations: China, 2004-2013, Environ. Health Perspect., 124, 184-192, 10.1289/ehp.1409481, 2016.
Mantas, E., Remoundaki, E., Halari, I., Kassomenos, P., Theodosi, C., Hatzikioseyian, A., and Mihalopoulos, N.: Mass closure and source apportionment of $PM_{2.5}$ by Positive Matrix Factorization analysis in urban Mediterranean environment, Atmospheric Environment, 94, 154-163, 10.1016/j.atmosenv.2014.05.002, 2014.
Meng, Z. Y., Lin, W. L., Jiang, X. M., Yan, P., Wang, Y., Zhang, Y. M., Jia, X. F., and Yu, X. L.: Characteristics of atmospheric ammonia over Beijing, China, Atmospheric Chemistry and Physics, 11, 6139-6151, 10.5194/acp-11-6139-2011, 2011.
Nel, A.: Air pollution-related illness: Effects of particles, Science, 308, 804-806, 10.1126/science.1108752, 2005.
Nie, W., Ding, A., Wang, T., Kerminen, V. M., George, C., Xue, L., Wang, W., Zhang, Q., Petaja, T., Qi, X., Gao, X., Wang, X., Yang, X., Fu, C., and Kulmala, M.: Polluted dust promotes new particle formation and growth, Scientific reports, 4, 6634, 10.1038/srep06634, 2014.
Peplow, M.: Beijing smog contains witches' brew of microbes, Nature, doi, 10, 2014.
Poschl, U.: Atmospheric aerosols: composition, transformation, climate and health effects, Angew Chem Int Ed Engl, 44, 7520-7540, 10.1002/anie.200501122, 2005.
Quan, J., Tie, X., Zhang, Q., Liu, Q., Li, X., Gao, Y., and Zhao, D.: Characteristics of heavy aerosol pollution during the 2012–2013 winter in Beijing, China, Atmospheric Environment, 88, 83-89, 10.1016/j.atmosenv.2014.01.058, 2014.
Ravishankara, A.: Heterogeneous and multiphase chemistry in the troposphere, Science, 276, 1058-1065, 1997.
Revuelta, C. C., de la Fuente Santiago, E., and Vázquez, J. A. R.: Characterization of Polycyclic Aromatic Hydrocarbons in Emissions from Coal-Fired Power Plants: The Influence of Operation Parameters, Environmental Technology, 20, 61-68, 10.1080/09593332008616793, 1999.
Shah, S. D., Cocker, D. R., Miller, J. W., and Norbeck, J. M.: Emission Rates of Particulate Matter and Elemental and Organic Carbon from In-Use Diesel Engines, Environ. Sci. Technol., 38, 2544-2550, 10.1021/es0350583, 2004.
Shapiro, J. B., Simpson, H. J., Griffin, K. L., and Schuster, W. S. F.: Precipitation chloride at West Point, NY: Seasonal patterns and possible contributions from non-seawater sources, Atmospheric

672 Environment, 41, 2240-2254, 10.1016/j.atmosenv.2006.03.049, 2007.
673 Shen, R., Schäfer, K., Schnelle-Kreis, J., Shao, L., Norra, S., Kramar, U., Michalke, B., Abbaszade,
674 G., Streibel, T., Fricker, M., Chen, Y., Zimmermann, R., Emeis, S., and Schmid, H. P.:
675 Characteristics and sources of PM in seasonal perspective – A case study from one year
676 continuously sampling in Beijing, Atmospheric Pollution Research, 7, 235-248,
677 10.1016/j.apr.2015.09.008, 2016.
678 Song, H., Shang, J., Zhu, T., Zhao, L., and Ye, J. H.: Heterogeneous Oxidation of SO_2 by Ozone
679 on the Surface of Black Carbon Particles, Chem. J. Chin. Univ. Chin., 33, 2295-2302,
680 10.7503/cjcu20120024, 2012.
681 Sun, Y. L., Wang, Z. F., Fu, P. Q., Yang, T., Jiang, Q., Dong, H. B., Li, J., and Jia, J. J.: Aerosol
682 composition, sources and processes during wintertime in Beijing, China, Atmospheric Chemistry
683 and Physics, 13, 4577-4592, 10.5194/acp-13-4577-2013, 2013.
684 Tan, J., Duan, J., Zhen, N., He, K., and Hao, J.: Chemical characteristics and source of
685 size-fractionated atmospheric particle in haze episode in Beijing, Atmospheric Research, 167,
686 24-33, 10.1016/j.atmosres.2015.06.015, 2016.
687 Tang, G. Q., Chao, N., Wang, Y. S., and Chen, J. S.: Vehicular emissions in China in 2006 and
688 2010, Journal of Environmental Sciences, 48, 179-192, 10.1016/j.jes.2016.01.031, 2016.
689 Tao, M., Chen, L., Su, L., and Tao, J.: Satellite observation of regional haze pollution over the
690 North China Plain, Journal of Geophysical Research: Atmospheres, 117, 10.1029/2012jd017915,
691 2012.
692 Taylor, S. R.: Trace element abundances and the chondritic earth model, Geochimica Et
693 Cosmochimica Acta, 28, 1989-1998, 10.1016/0016-7037(64)90142-5, 1964.
694 Tian, S., Pan, Y., Liu, Z., Wen, T., and Wang, Y.: Size-resolved aerosol chemical analysis of
695 extreme haze pollution events during early 2013 in urban Beijing, China, J Hazard Mater, 279,
696 452-460, 10.1016/j.jhazmat.2014.07.023, 2014.
697 Underwood, G. M., Song, C. H., Phadnis, M., Carmichael, G. R., and Grassian, V. H.:
698 Heterogeneous reactions of NO_2 and HNO_3 on oxides and mineral dust: A combined laboratory
699 and modeling study, Journal of Geophysical Research: Atmospheres, 106, 18055-18066,
700 10.1029/2000jd900552, 2001.
701 Van Eyk, P. J., Ashman, P. J., and Nathan, G. J.: Mechanism and kinetics of sodium release from
702 brown coal char particles during combustion, Combustion and Flame, 158, 2512-2523,
703 10.1016/j.combustflame.2011.05.005, 2011.
704 Wang, G., Zhang, R., Gomez, M. E., Yang, L., Levy Zamora, M., Hu, M., Lin, Y., Peng, J., Guo,
705 S., Meng, J., Li, J., Cheng, C., Hu, T., Ren, Y., Wang, Y., Gao, J., Cao, J., An, Z., Zhou, W., Li, G.,
706 Wang, J., Tian, P., Marrero-Ortiz, W., Secrest, J., Du, Z., Zheng, J., Shang, D., Zeng, L., Shao, M.,
707 Wang, W., Huang, Y., Wang, Y., Zhu, Y., Li, Y., Hu, J., Pan, B., Cai, L., Cheng, Y., Ji, Y., Zhang, F.,
708 Rosenfeld, D., Liss, P. S., Duce, R. A., Kolb, C. E., and Molina, M. J.: Persistent sulfate formation
709 from London Fog to Chinese haze, Proceedings of the National Academy of Sciences of the
710 United States of America, 2016.
711 Wang, H., Zhou, Y., Zhuang, Y., Wang, X., and Hao, Z.: Characterization of $PM_{2.5}$/$PM_{2.5\text{-}10}$ and
712 source tracking in the juncture belt between urban and rural areas of Beijing, Chinese Science
713 Bulletin, 54, 2506-2515, 10.1007/s11434-009-0021-x, 2009.
714 Wang, H. L., Hao, Z. P., Zhuang, Y. H., Wang, W., and Liu, X. Y.: Characterization of inorganic
715 components of size-segregated particles in the flue gas of a coal-fired power plant, Energy &

Fuels, 22, 1636-1640, 10.1021/ef700527y, 2008.
Wang, Y., Zhuang, G. S., Tang, A. H., Yuan, H., Sun, Y. L., Chen, S. A., and Zheng, A. H.: The ion chemistry and the source of $PM_{2.5}$ aerosol in Beijing, Atmospheric Environment, 39, 3771-3784, 10.1016/j.atmosenv.2005.03.013, 2005.
Wang, Y., Yao, L., Wang, L., Liu, Z., Ji, D., Tang, G., Zhang, J., Sun, Y., Hu, B., and Xin, J.: Mechanism for the formation of the January 2013 heavy haze pollution episode over central and eastern China, Science China Earth Sciences, 57, 14-25, 10.1007/s11430-013-4773-4, 2013.
Wen, W., Cheng, S., Chen, X., Wang, G., Li, S., Wang, X., and Liu, X.: Impact of emission control on $PM_{2.5}$ and the chemical composition change in Beijing-Tianjin-Hebei during the APEC summit 2014, Environmental science and pollution research international, 23, 4509-4521, 10.1007/s11356-015-5379-5, 2016.
Wu, L. Y., Tong, S. R., Wang, W. G., and Ge, M. F.: Effects of temperature on the heterogeneous oxidation of sulfur dioxide by ozone on calcium carbonate, Atmospheric Chemistry and Physics, 11, 6593-6605, 10.5194/acp-11-6593-2011, 2011.
Wu, S., Deng, F., Wei, H., Huang, J., Wang, X., Hao, Y., Zheng, C., Qin, Y., Lv, H., Shima, M., and Guo, X.: Association of cardiopulmonary health effects with source-appointed ambient fine particulate in Beijing, China: a combined analysis from the Healthy Volunteer Natural Relocation (HVNR) study, Environ Sci Technol, 48, 3438-3448, 10.1021/es404778w, 2014.
Xu, S. S., Liu, W. X., and Tao, S.: Emission of polycyclic aromatic hydrocarbons in China, Environ. Sci. Technol., 40, 702-708, 10.1021/es0517062, 2006.
Xu, W. Y., Zhao, C. S., Ran, L., Deng, Z. Z., Liu, P. F., Ma, N., Lin, W. L., Xu, X. B., Yan, P., He, X., Yu, J., Liang, W. D., and Chen, L. L.: Characteristics of pollutants and their correlation to meteorological conditions at a suburban site in the North China Plain, Atmospheric Chemistry and Physics, 11, 4353-4369, 10.5194/acp-11-4353-2011, 2011.
Yang, F., Tan, J., Zhao, Q., Du, Z., He, K., Ma, Y., Duan, F., Chen, G., and Zhao, Q.: Characteristics of $PM_{2.5}$ speciation in representative megacities and across China, Atmospheric Chemistry and Physics, 11, 5207-5219, 10.5194/acp-11-5207-2011, 2011.
Yang, X., Geng, C., Sun, X., Yang, W., Wang, X., and Chen, J.: Characteristics of particulate-bound polycyclic aromatic hydrocarbons emitted from industrial grade biomass boilers, J Environ Sci (China), 40, 28-34, 10.1016/j.jes.2015.09.010, 2016.
Yang, Y. R., Liu, X. G., Qu, Y., An, J. L., Jiang, R., Zhang, Y. H., Sun, Y. L., Wu, Z. J., Zhang, F., Xu, W. Q., and Ma, Q. X.: Characteristics and formation mechanism of continuous hazes in China: a case study during the autumn of 2014 in the North China Plain, Atmospheric Chemistry and Physics, 15, 8165-8178, 10.5194/acp-15-8165-2015, 2015.
Yao, L., Yang, L., Chen, J., Wang, X., Xue, L., Li, W., Sui, X., Wen, L., Chi, J., Zhu, Y., Zhang, J., Xu, C., Zhu, T., and Wang, W.: Characteristics of carbonaceous aerosols: Impact of biomass burning and secondary formation in summertime in a rural area of the North China Plain, The Science of the total environment, 557-558, 520-530, 10.1016/j.scitotenv.2016.03.111, 2016.
Yu, L. D., Wang, G. F., Zhang, R. J., Zhang, L. M., Song, Y., Wu, B. B., Li, X. F., An, K., and Chu, J. H.: Characterization and Source Apportionment of $PM_{2.5}$ in an Urban Environment in Beijing, Aerosol and Air Quality Research, 13, 574-583, 10.4209/aaqr.2012.07.0192, 2013.
Zhang, H., Wang, S., Hao, J., Wang, X., Wang, S., Chai, F., and Li, M.: Air pollution and control action in Beijing, Journal of Cleaner Production, 112, 1519-1527, 10.1016/j.jclepro.2015.04.092, 2016.

760 Zhang, Q., He, K. B., and Huo, H.: Cleaning China's air, Nature, 484, 161-162, 2012.
761 Zhang, R., Jing, J., Tao, J., Hsu, S. C., Wang, G., Cao, J., Lee, C. S. L., Zhu, L., Chen, Z., Zhao, Y.,
762 and Shen, Z.: Chemical characterization and source apportionment of $PM_{2.5}$ in Beijing: seasonal
763 perspective, Atmospheric Chemistry and Physics, 13, 7053-7074, 10.5194/acp-13-7053-2013,
764 2013.
765 Zhang, R., Wang, G., Guo, S., Zamora, M. L., Ying, Q., Lin, Y., Wang, W., Hu, M., and Wang, Y.:
766 Formation of urban fine particulate matter, Chem Rev, 115, 3803-3855,
767 10.1021/acs.chemrev.5b00067, 2015.
768 Zhang, X. Y., Gong, S. L., Shen, Z. X., Mei, F. M., Xi, X. X., Liu, L. C., Zhou, Z. J., Wang, D.,
769 Wang, Y. Q., and Cheng, Y.: Characterization of soil dust aerosol in China and its transport and
770 distribution during 2001 ACE-Asia: 1. Network observations, Journal of Geophysical Research:
771 Atmospheres, 108, 10.1029/2002jd002632, 2003.
772 Zhang, Y., Schauer, J. J., Zhang, Y., Zeng, L., Wei, Y., Liu, Y., and Shao, M.: Characteristics of
773 particulate carbon emissions from real-world Chinese coal combustion, Environ. Sci. Technol., 42,
774 5068-5073, 10.1021/es7022576, 2008.
775 Zhang, Z., Wang, H., Chen, D., Li, Q., Thai, P., Gong, D., Li, Y., Zhang, C., Gu, Y., Zhou, L.,
776 Morawska, L., and Wang, B.: Emission characteristics of volatile organic compounds and their
777 secondary organic aerosol formation potentials from a petroleum refinery in Pearl River Delta,
778 China, The Science of the total environment, 584-585, 1162-1174,
779 10.1016/j.scitotenv.2017.01.179, 2017.
780 Zhao, P. S., Dong, F., He, D., Zhao, X. J., Zhang, X. L., Zhang, W. Z., Yao, Q., and Liu, H. Y.:
781 Characteristics of concentrations and chemical compositions for $PM_{2.5}$ in the region of Beijing,
782 Tianjin, and Hebei, China, Atmospheric Chemistry and Physics, 13, 4631-4644,
783 10.5194/acp-13-4631-2013, 2013a.
784 Zhao, P. S., Dong, F., Yang, Y. D., He, D., Zhao, X. J., Zhang, W. Z., Yao, Q., and Liu, H. Y.:
785 Characteristics of carbonaceous aerosol in the region of Beijing, Tianjin, and Hebei, China,
786 Atmospheric Environment, 71, 389-398, 10.1016/j.atmosenv.2013.02.010, 2013b.
787 Zhao, X. J., Zhao, P. S., Xu, J., Meng, W., Pu, W. W., Dong, F., He, D., and Shi, Q. F.: Analysis of
788 a winter regional haze event and its formation mechanism in the North China Plain, Atmospheric
789 Chemistry and Physics, 13, 5685-5696, 10.5194/acp-13-5685-2013, 2013.
790 Zhao, Y., Ma, Q., Liu, Y., and He, H.: Influence of sulfur in fuel on the properties of diffusion
791 flame soot, Atmospheric Environment, 142, 383-392, 10.1016/j.atmosenv.2016.08.001, 2016.
792 Zheng, B., Zhang, Q., Zhang, Y., He, K. B., Wang, K., Zheng, G. J., Duan, F. K., Ma, Y. L., and
793 Kimoto, T.: Heterogeneous chemistry: a mechanism missing in current models to explain
794 secondary inorganic aerosol formation during the January 2013 haze episode in North China,
795 Atmospheric Chemistry and Physics, 15, 2031-2049, 10.5194/acp-15-2031-2015, 2015.
796 Zheng, G. J., Duan, F. K., Su, H., Ma, Y. L., Cheng, Y., Zheng, B., Zhang, Q., Huang, T., Kimoto,
797 T., Chang, D., Pöschl, U., Cheng, Y. F., and He, K. B.: Exploring the severe winter haze in Beijing:
798 the impact of synoptic weather, regional transport and heterogeneous reactions, Atmospheric
799 Chemistry and Physics, 15, 2969-2983, 10.5194/acp-15-2969-2015, 2015.
800 Zong, Z., Wang, X., Tian, C., Chen, Y., Qu, L., Ji, L., Zhi, G., Li, J., and Zhang, G.: Source
801 apportionment of $PM_{2.5}$ at a regional background site in North China using PMF linked with
802 radiocarbon analysis: insight into the contribution of biomass burning, Atmospheric Chemistry
803 and Physics, 16, 11249-11265, 10.5194/acp-16-11249-2016, 2016.

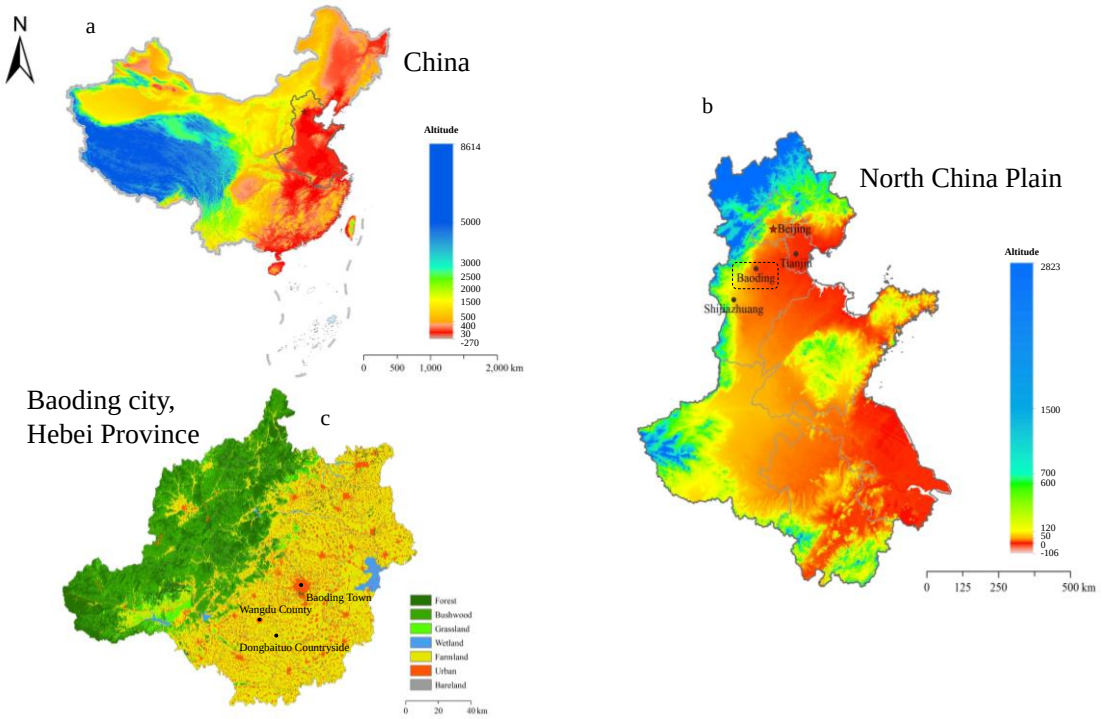

Figure 1. China (a), the North China Plain (b) and Baoding city in Hebei Province (c). The locations of sampling sites (BJ, BD, WD and DBT) as well as Tianjin municipality and Shijiazhuang as provincial capital of Hebei are marked.

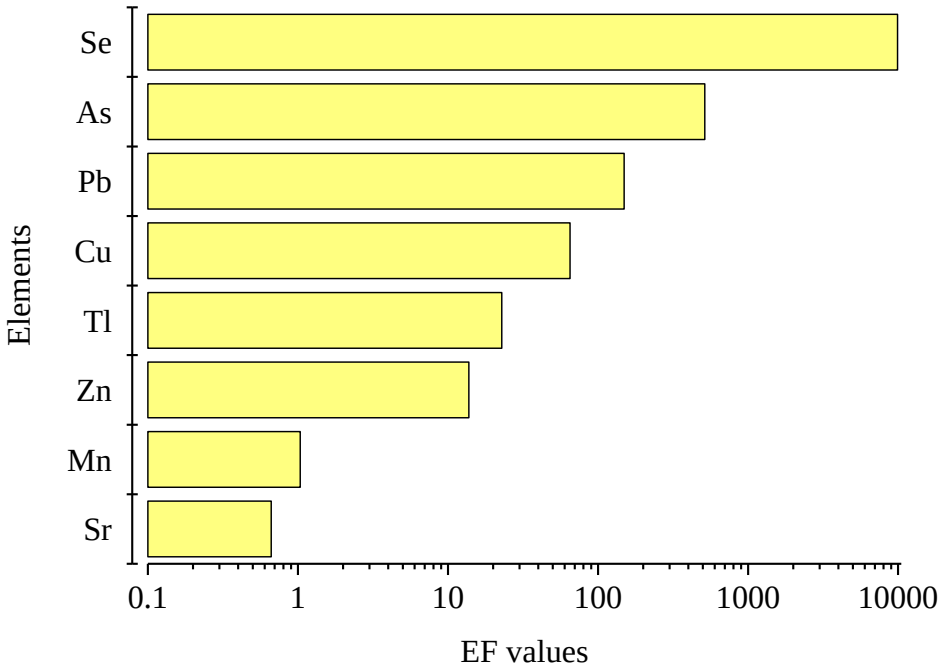

Figure 2. Enrichment factor values for trace elements in $PM_{2.5}$.

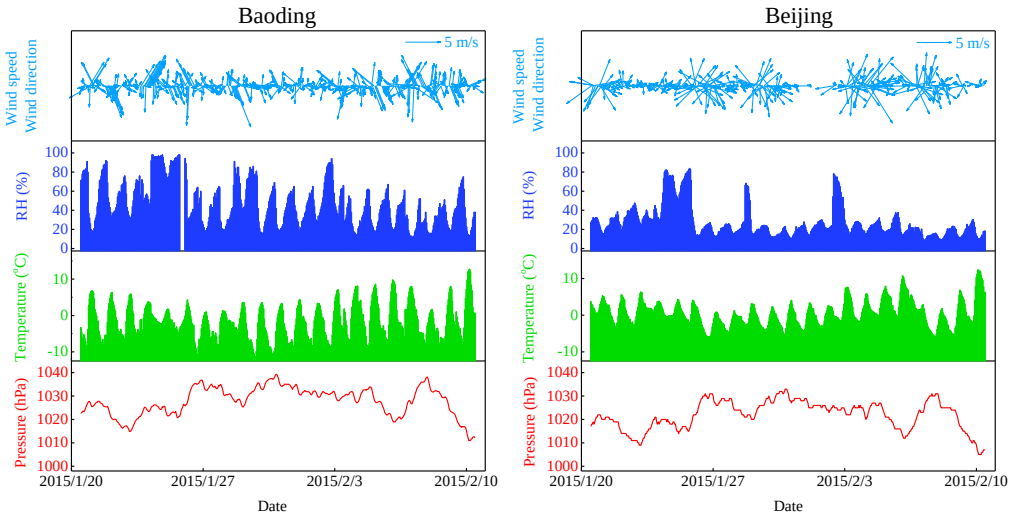

Figure 3. The wind speed, wind direction, RH, temperature and barometric pressure at BD and BJ during the sampling period in the winter of 2015.

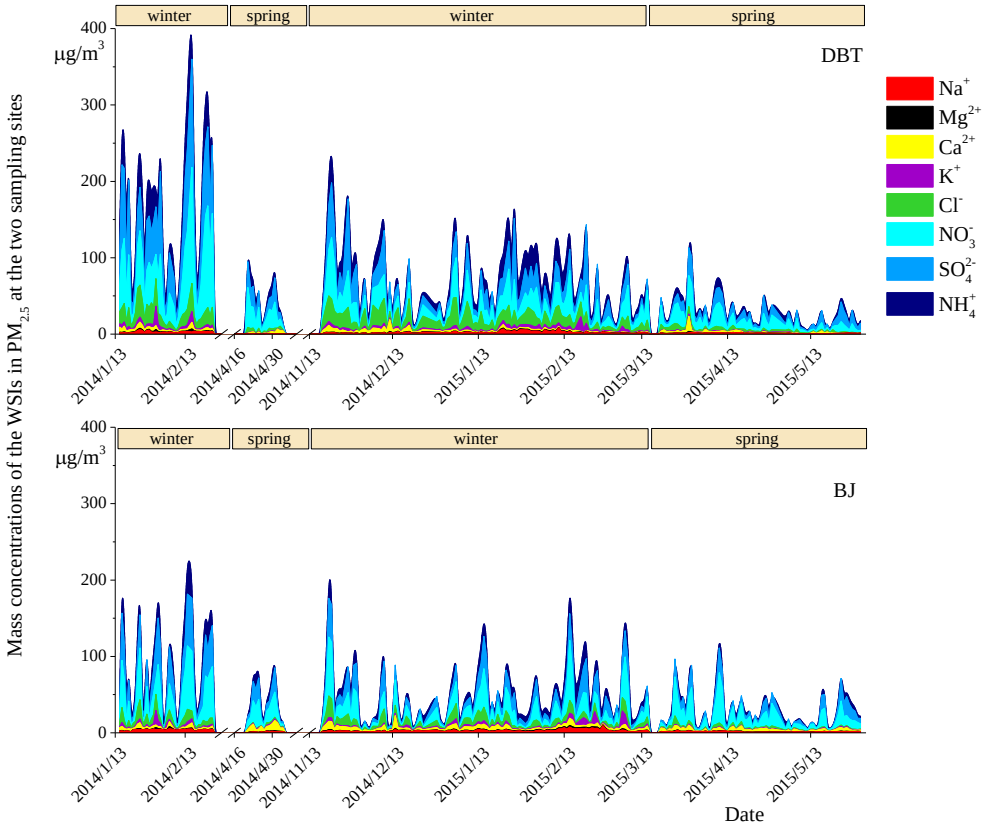

Figure 4. The mass concentrations of the WSIs in $PM_{2.5}$ at DBT and BJ during the sampling period in the winters and springs of 2014-2015.

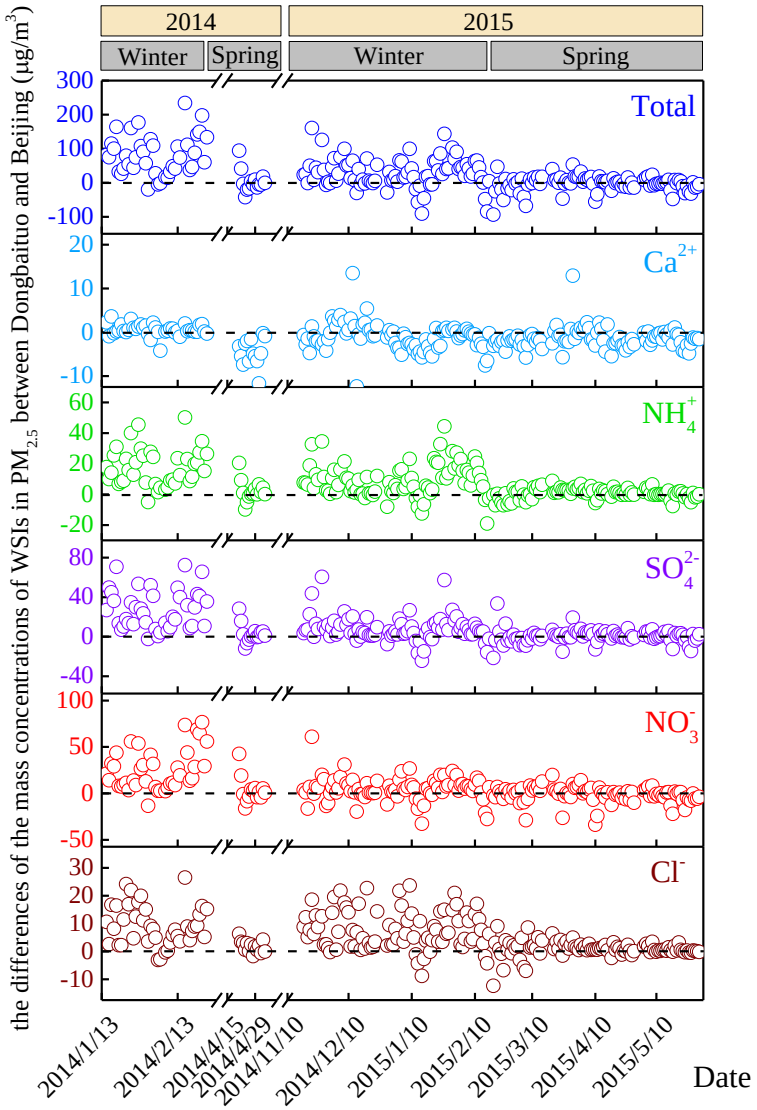

816

817 **Figure 5.** The D-values of the mass concentrations of WSIs in $PM_{2.5}$ between DBT and BJ during

818 the sampling period in the winters and springs of 2014-2015.

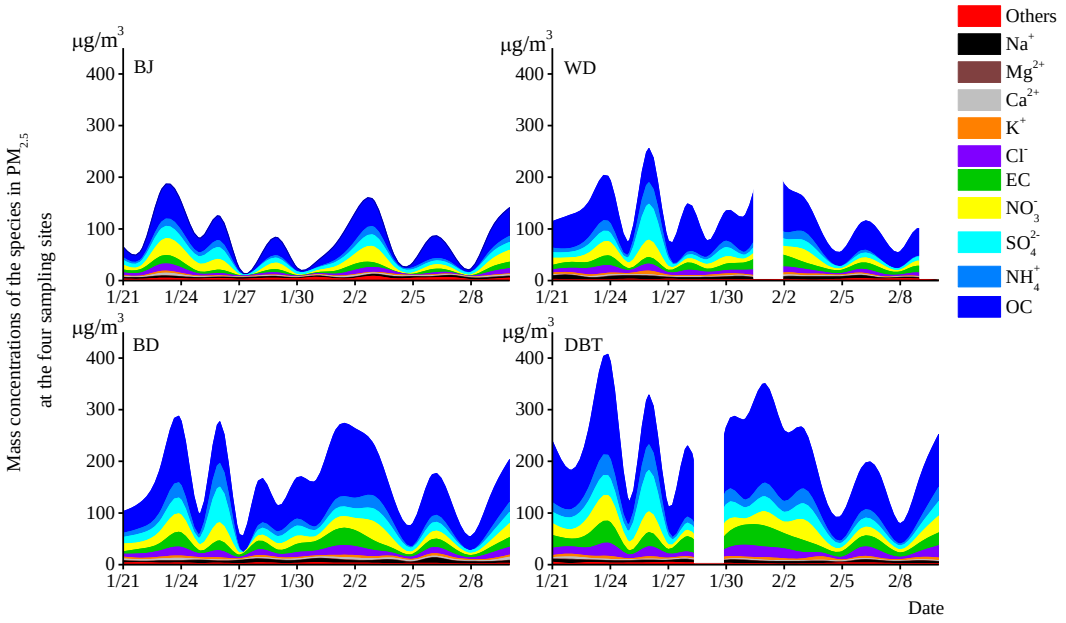

819

820 **Figure 6.** Daily variation of the species in $PM_{2.5}$ at the four sampling sites during the sampling
821 period in the winter of 2015.

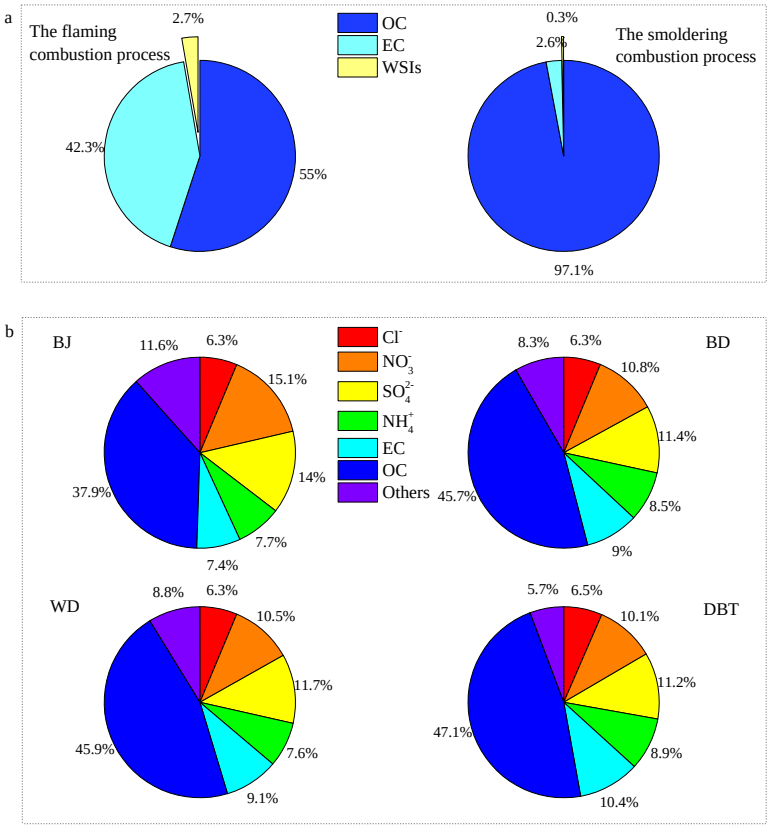

822

823 **Figure 7.** The mass proportions of OC, EC and WSIs from residential coal combustion under the
824 flaming and smoldering combustion processes (a), and the average mass proportions of the typical

species in $PM_{2.5}$ at the four sampling sites during the sampling period in the winter of 2015 (b).

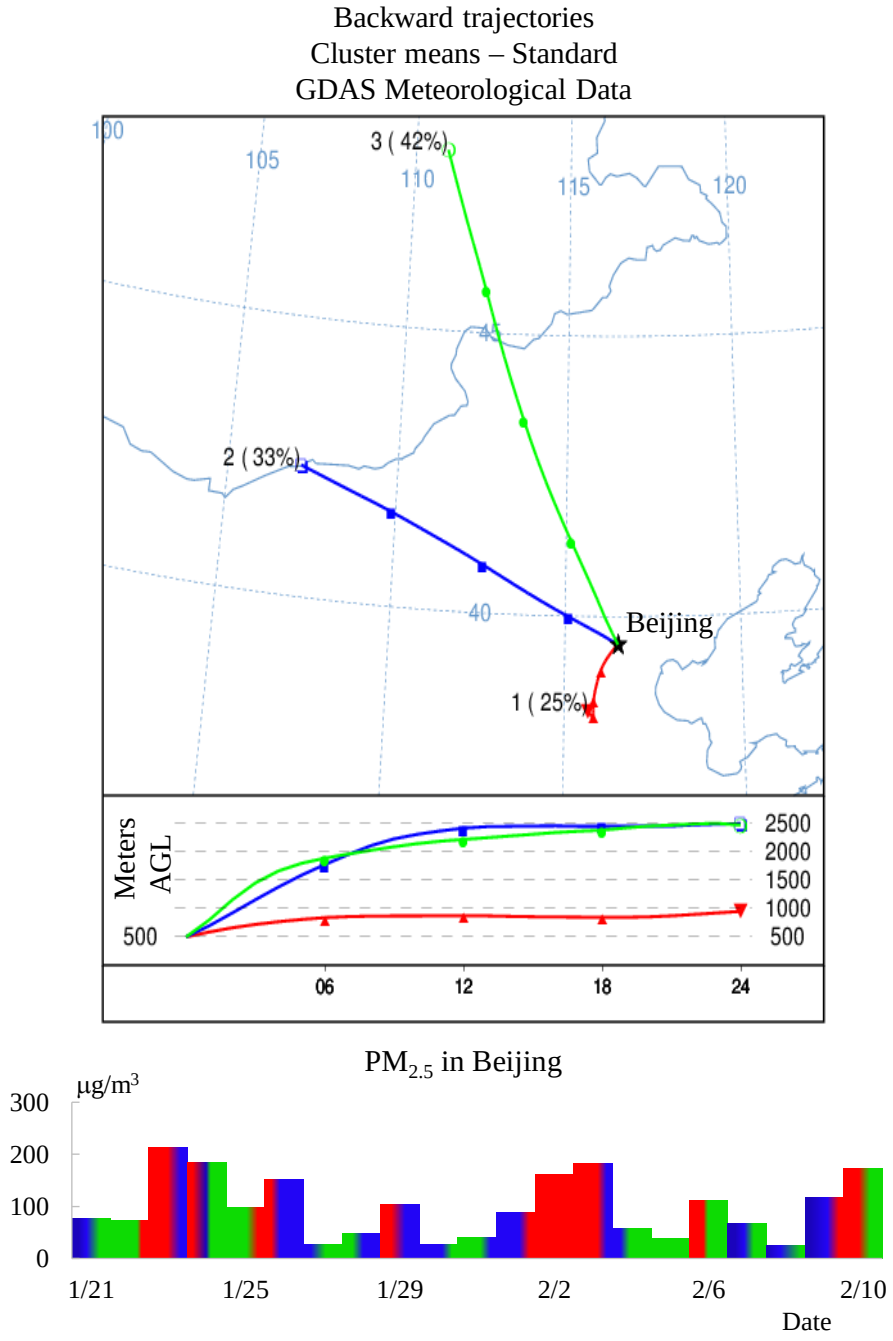

Figure 8. The back trajectory cluster analysis and the corresponding $PM_{2.5}$ concentrations in Beijing during the sampling period in the winter of 2015.

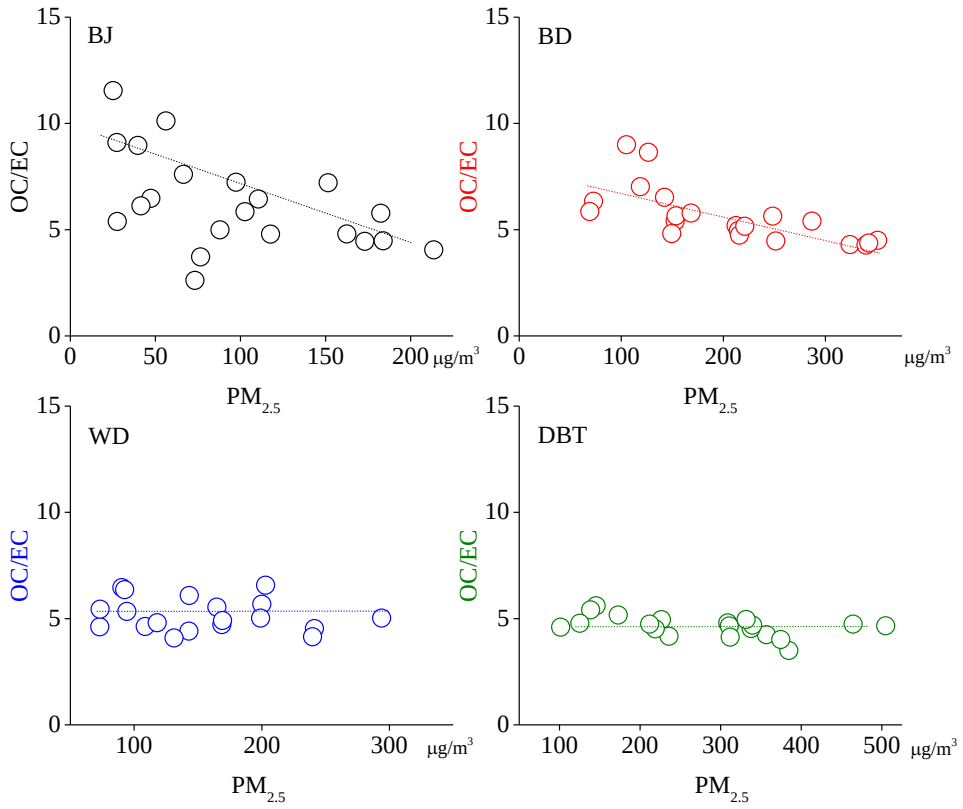

Figure 9. The correlations between the OC/EC ratios and the $PM_{2.5}$ concentrations at the four sampling sites during the sampling period in the winter of 2015.

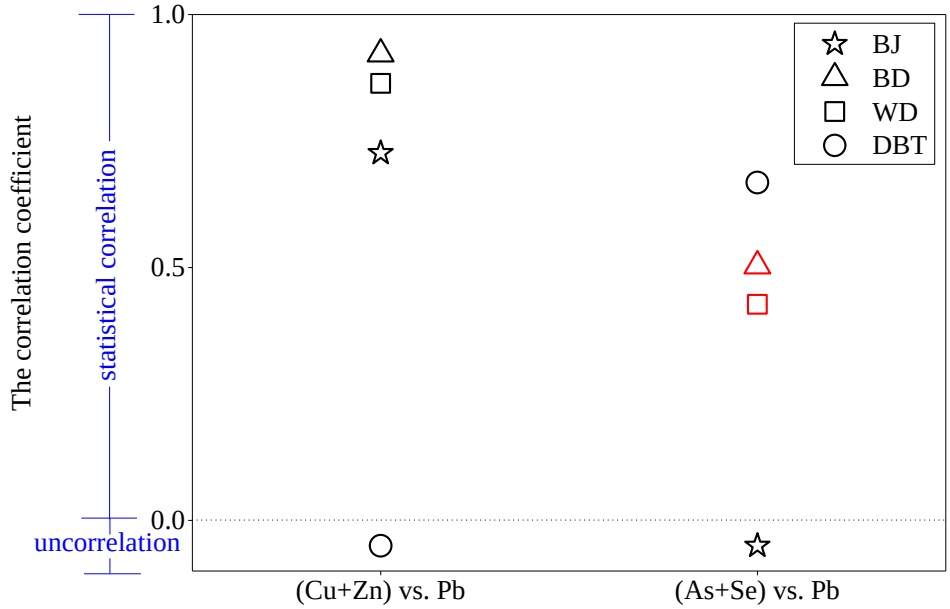

Figure 10. The statistical correlations for [Cu+Zn] vs. [Pb] and [As+Se] vs. [Pb] in $PM_{2.5}$ at the four sampling sites during the sampling period in the winter of 2015. The uncorrelated results are

836 also marked below zero of Y axis. The red and black symbols represent for $p < 0.05$ and $p < 0.01$,
837 respectively.

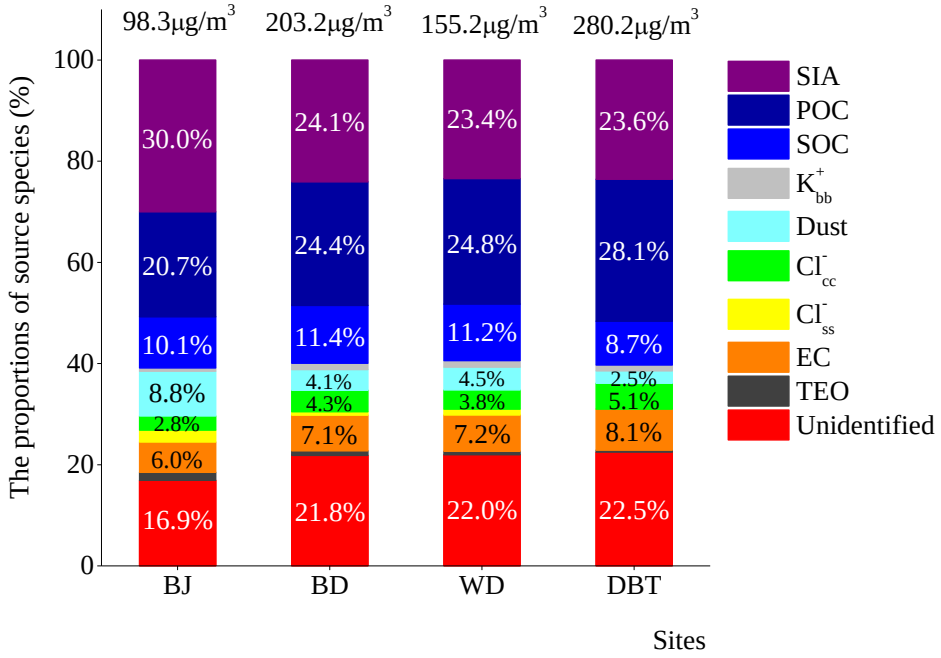

838
839 **Figure 11.** The proportions of source species under the constructed chemical mass closures for
840 $PM_{2.5}$ at the four sampling sites during the sampling period in the winter of 2015. Average mass
841 concentrations of $PM_{2.5}$ at each sampling site, including all of source species and unidentified
842 fractions, are also marked at the top of bar charts.

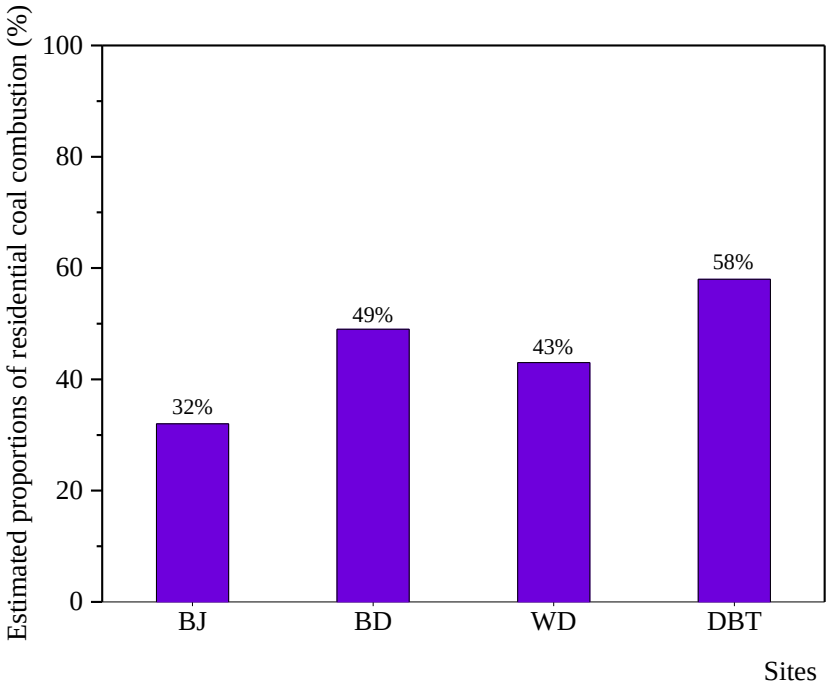

843

Figure 12. The estimated contributions of coal combustion to the $PM_{2.5}$ at the four sampling sites during the sampling period in the winter of 2015.

Table 1. The average mass concentrations of WSIs in $PM_{2.5}$ at DBT and BJ during the sampling period in the winters and springs of 2014-2015 ($\mu g\ m^{-3}$).

WSIs	spring		winter	
	DBT	BJ	DBT	BJ
Na^+	1.0 ±0.5	1.4 ±0.5	2.4 ±1.3	3.1 ±1.4
Mg^{2+}	0.2 ±0.2	0.3 ±0.2	0.7 ±0.5	0.8 ±0.7
Ca^{2+}	1.7 ±2.4	3.4 ±2.5	2.6 ±2.1	3.4 ±2.3
K^+	0.5 ±0.5	0.7 ±0.4	3.2 ±3.0	3.0 ±6.0
NH_4^+	6.1 ±5.1	4.8 ±4.7	23.1 ±17.9	13.2 ±11.6
NO_3^-	12.5 ±11.2	13.6 ±13.2	28.4 ±28.0	19.0 ±20.0
SO_4^{2-}	10.5 ±8.2	9.2 ±8.6	29.0 ±28.1	17.4 ±16.5
Cl^-	2.9 ±2.2	1.8 ±1.6	14.1 ±9.4	7.2 ±6.0
Total	35.3 ±26.7	35.1 ±28.7	103.3 ±81.3	67.0 ±55.2

Table 2. The average mass concentrations (Mean ±SD) of $PM_{2.5}$ species, NO_2 and SO_2 at the four sampling sites during the sampling period in the winter of 2015 ($\mu g\ m^{-3}$).

Species	BJ	BD	WD	DBT
Na^+	2.5 ±0.7	4.8 ±2.0	4.5 ±1.7	4.3 ±1.2
Mg^{2+}	0.3 ±0.1	0.4 ±0.1	0.3 ±0.1	0.4 ±0.2
Ca^{2+}	1.8 ±0.9	2.6 ±0.8	1.7 ±0.6	2.0 ±0.8
K^+	0.7 ±0.8	2.5 ±1.0	2.0 ±1.4	3.1 ±1.3
NH_4^+	6.0 ±5.0	13.3 ±11.0	9.3 ±9.5	18.7 ±11.7
NO_3^-	11.7 ±10.1	16.6 ±10.3	13.0 ±8.2	21.0 ±12.2
SO_4^{2-}	11.2 ±6.5	18.1 ±14.1	14.5 ±14.5	24.1 ±16.1
Cl^-	5.0 ±3.6	9.5 ±4.2	7.8 ±3.5	13.4 ±6.0
OC	28.6 ±19.6	70.2 ±31.2	57.2 ±21.3	100.0 ±42.9
EC	5.5 ±4.5	13.5 ±7.8	11.4 ±4.7	21.6 ±10.2
Al	0.6 ±0.8	0.6 ±0.1	0.5 ±0.2	0.5 ±0.1
Mn	0.1 ±0.1	0.1 ±0.1	0.1 ±0.1	0.2 ±0.3
Fe	2.1 ±0.8	0.6 ±0.2	0.8 ±0.6	1.3 ±0.6
Cu	0.6 ±0.3	0.3 ±0.1	0.2 ±0.1	0.1 ±0.1
Zn	0.1 ±0.1	0.2 ±0.1	0.1 ±0.1	0.1 ±0.1
As	0.1 ±0.1	0.3 ±0.1	0.2 ±0.1	0.1 ±0.1
Se	0.1 ±0.0	0.1 ±0.1	0.1 ±0.0	0.1 ±0.0
Sr	0.0 ±0.0	0.1 ±0.0	0.0 ±0.0	0.0 ±0.0
Tl	0.0 ±0.0	0.0 ±0.0	0.0 ±0.0	0.0 ±0.0
Pb	0.2 ±0.2	0.4 ±0.3	0.2 ±0.1	0.3 ±0.1
The total	80.1 ±47.7	159.5 ±70.3	121.7 ±51.8	218.4 ±87.1
NO_2	36.5 ±17.4	60.4 ±23.4	76.1 ±19.2	-
SO_2	63.9 ±31.7	181.7 ±62.4	101.3 ±39.4	-

Table 3. The emission factors (Mean ± SD) (g kg^{-1} coal) of OC and EC from residential coal combustion during the flaming combustion process, the smoldering combustion process and the entire combustion process.

Emission factors	the flaming combustion process	the smoldering combustion process	the entire combustion process
OC	1.83 ± 1.19	17.11 ± 0.79	10.99 ± 0.95
EC	1.40 ± 0.11	0.46 ± 0.03	0.84 ± 0.06

Table 4. The correlations of several typical species in $PM_{2.5}$ at the four sampling sites during the sampling period in the winter of 2015.

n=21	BJ								
	Mg^{2+}	Ca^{2+}	K^+	Cl^-	NO_3^-	SO_4^{2-}	NH_4^+	OC	EC
Mg^{2+}	1								
Ca^{2+}	0.895**	1							
K^+	0.634**	0.862**	1						
Cl^-	0.856**	0.899**	0.791**	1					
NO_3^-	0.803**	0.768**	0.637**	0.905**	1				
SO_4^{2-}	0.679**	0.660**	0.590**	0.804**	0.950**	1			
NH_4^+	0.718**	0.667**	0.543*	0.834**	0.971**	0.959**	1		
OC	0.845**	0.751**	0.560**	0.848**	0.919**	0.838**	0.895**	1	
EC	0.849**	0.851**	0.679**	0.932**	0.877**	0.769**	0.823**	0.936**	1
n=21	BD								
	Mg^{2+}	Ca^{2+}	K^+	Cl^-	NO_3^-	SO_4^{2-}	NH_4^+	OC	EC
Mg^{2+}	1								
Ca^{2+}	0.805**	1							
K^+	0.697**	0.556**	1						
Cl^-	0.714**	0.659**	0.789**	1					
NO_3^-	0.554**	0.560**	0.675**	0.757**	1				
SO_4^{2-}	0.022	0.107	0.491*	0.499*	0.764**	1			
NH_4^+	0.315	0.331	0.659**	0.721**	0.920**	0.941**	1		
OC	0.743**	0.576**	0.705**	0.936**	0.674**	0.369	0.614**	1	
EC	0.698**	0.560**	0.702**	0.939**	0.660**	0.410	0.633**	0.984**	1
n=19	WD								
	Mg^{2+}	Ca^{2+}	K^+	Cl^-	NO_3^-	SO_4^{2-}	NH_4^+	OC	EC
Mg^{2+}	1								
Ca^{2+}	0.897**	1							
K^+	0.226	0.457*	1						
Cl^-	0.532*	0.663**	0.598**	1					
NO_3^-	0.468*	0.677**	0.712**	0.796**	1				
SO_4^{2-}	0.097	0.358	0.874**	0.552*	0.770**	1			
NH_4^+	0.306	0.563**	0.906**	0.735**	0.901**	0.945**	1		
OC	0.463*	0.543*	0.372	0.816**	0.471*	0.222	0.581*	1	
EC	0.553*	0.638**	0.339	0.763**	0.510*	0.214	0.565*	0.925**	1

n=20	DBT								
	Mg^{2+}	Ca^{2+}	K^{+}	Cl^{-}	NO_3^{-}	SO_4^{2-}	NH_4^{+}	OC	EC
Mg^{2+}	1								
Ca^{2+}	0.721**	1							
K^{+}	0.191	0.407	1						
Cl^{-}	-0.061	0.316	0.519*	1					
NO_3^{-}	-0.241	0.161	0.579**	0.642**	1				
SO_4^{2-}	-0.133	0.109	0.458*	0.482*	0.744**	1			
NH_4^{+}	-0.223	0.125	0.558*	0.697**	0.928**	0.914**	1		
OC	0.067	0.159	0.419	0.772**	0.570**	0.293	0.557*	1	
EC	0.051	0.169	0.419	0.838**	0.585**	0.400	0.624**	0.977**	1

*, ** represent for $p < 0.05$ and $p < 0.01$, respectively.

Table 5. The correlations between [Zn] vs. [Cu] and [As] vs. [Se] in $PM_{2.5}$ at the four sampling sites during the sampling period in the winter of 2015.

Elements	BJ (n=21)	BD (n=21)	WD (n=19)	DBT (n=20)
[Zn] vs. [Cu]	0.607**	0.479*	0.620*	0.659**
[As] vs. [Se]	0.662**	0.664**	0.959**	0.871**

*, ** represent for $p < 0.05$ and $p < 0.01$, respectively.